Trends in the Athermal Entropy of Mixing of Polymer Solutions

DATASET *in* MACROMOLECULES · MARCH 2014

Impact Factor: 5.8 · DOI: 10.1021/ma402593m

3 AUTHORS, INCLUDING:

Amir Vahid
Northwestern University
28 PUBLICATIONS **66** CITATIONS
SEE PROFILE

Jarrell Richard Elliott
University of Akron
100 PUBLICATIONS **1,154** CITATIONS
SEE PROFILE

Macromolecules

Article

pubs.acs.org/Macromolecules

Trends in the Athermal Entropy of Mixing of Polymer Solutions

Amir Vahid,[†] Neil H. Gray,[‡] and J. Richard Elliott[†,*]

[†]Chemical and Biomolecular Engineering Department The University of Akron, Akron Ohio 44325 United States

[‡]Chemstations Inc., 2901 Wilcrest Drive, Houston Texas 77042 United States

Supporting Information

ABSTRACT: Polymeric mixtures of hydrocarbons and alcohols have been simulated with discontinuous potential models to characterize the Helmholtz energy of the repulsive reference fluids. This quantity is equivalent to the athermal mixture entropy. The reference compressibility factor and Helmholtz free energy have been correlated for various molecular structures from single to infinite chain lengths. The mixtures included small *n*-alkanes, branched alkanes, aromatics, and alcohols, with polymeric molecules of: *n*-alkanes, ethyl-styrenes, ethyl-propylenes, and isoprenes. We find that the athermal entropy of mixing at constant packing fraction deviates significantly from ideality as the volume ratio increases, but the nonideality is fairly insensitive to structural details like branching and rings. Volume ratio alone does not provide a complete characterization, however. For example, a mixture of C40 and C80 would yield a small deviation whereas a mixture of C2 and C4 would provide a relatively large deviation. This observation leads to the introduction of a characteristic parameter in terms of entropy density, designated as an entropic solubility parameter. In both ideal and nonideal solutions, the trends still follow van der Waals (vdW) mixing. This leads to an accurate characterization of the entropic contribution to the χ parameter (χ^S) of Flory–Huggins theory for mixtures of all sizes, shapes, and compositions of molecular structures. A general rule is developed for predicting the athermal entropy of mixing based on knowledge of the volume ratios and entropic solubility parameter of the constituent molecules. The simulations are compared to Flory–Huggins (FH), group contribution lattice fluid theory (GCLF), statistical associating fluid theory (SAFT), Sanchez–Lacombe (SL), and Guggenheim-Staverman (GS) theories of polymer chains.

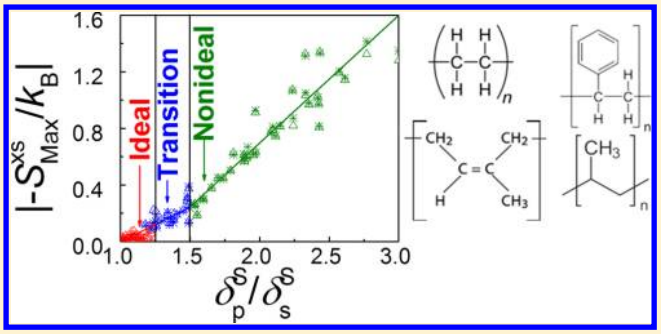

1. INTRODUCTION

The National Research Council (NRC) has identified computer-based molecular product design as a challenge for chemists, chemical and polymer engineers, and scientists.[1] One key to success is translating the molecular scale results into a form that can be used in a practical manner. Rather than simulating single state points or mixture equilibria, practical applications must provide results in a form that can be interpolated to any condition that may be encountered. Therefore, analytical formulas must be sought to quantitatively characterize results from both experiment and molecular simulation.

The excess entropy of mixing is fundamental to phase behavior, making it a primary consideration in thermodynamic modeling. Many analyses have focused on the entropy of mixing based on lattice models,[2−6] but relatively few have focused on off-lattice behavior.[7,8] Off-lattice methods are to be preferred when feasible because molecules distribute themselves throughout continuous space. While the computational efficiency that lattice models offer has been a key factor in the past, this justification is less substantial in a modern computing environment. The key question is whether the lattice models are sufficiently accurate to obviate the need for a detailed molecular simulation. We seek to address this question through the work presented here. An example of recent off-lattice work is provided by Alawneh and Henderson.[9,10] They have performed an extensive simulation and integral equation study to analyze the radial distribution functions of symmetric and highly asymmetric hard-sphere mixtures in the colloidal limit where the size ratio is large while the concentration of the large sphere is small. However, their work is only limited to hard spheres and the behavior of the excess entropy was not treated explicitly. Simulation studies of excess entropy of mixtures have been done by Mansoori et al.[11] for hard sphere mixtures. Gray and Elliott[12] presented results for mixtures over a limited range of size ratios, but these were never published. These results were summarized by Vahid et al.[13] An apparent inconsistency was observed by Vahid et al. when the trend was analyzed in the long chain limit.[13] That inconsistency has now been found to be unrelated to the entropy of mixing.

The primary property of interest in these analyses is the deviation of the entropy from ideal solution behavior. We refer to this property as the excess entropy of mixing, S^{xs}, consistent with the Gibbs excess energy of mixing that forms the basis of

Received: December 18, 2013
Revised: February 9, 2014
Published: February 26, 2014

phase behavior analysis. This property should not be confused with the (pure component) "excess entropy" that Dzugutov et al.[14] and Rosenfield et al.[15,16] have correlated with transport properties. We refer to that pure component property as the entropy departure function (deviation from ideal gas behavior).

The present work analyzes the excess entropy through molecular simulations of a broad range of compound types and sizes. We consider chain molecules composed of straight segments, rings, and branches mixed with solvents that may be spheres, chains, rings, or branches to probe the roles of surface to volume ratio in various contexts as well as size and entropic solubility parameter effects.

The molecular simulation technique applies discontinuous molecular dynamics (DMD) to hard core molecules composed of united atom fused spheres with conventional molecular details (i.e., bond lengths, bond angles, etc.), but no attractive contribution. DMD is uniquely suited to this particular analysis for several reasons. Soft core molecular models exhibit varying properties with temperature and the internal energy is nonzero. Softness leads to ambiguity when comparing various molecular sizes because small molecules tend to be relatively "softer". For example, this relative softness is particularly evident in the self-diffusivity at high temperature.[17] The overlaps of electron density induced by covalent bonds on all sides of an atom make it more difficult to penetrate than for a single atom in space. The complex implications of softness are also evident in the reference contribution to TPT when applying Lennard-Jones potential models.[18] Nonzero values of internal energy lead to imprecision; since the nonidealities tend to be small differences between large numbers, imprecision undermines any clear interpretation.

The remainder of this article is organized as follows. The concept of athermal and residual contributions to the entropy of mixing has been described in the next section. Details of the simulation methodology are presented in section 3. Succeeding sections present the analysis and results of the asymptotic trends for compressibility factor and entropy departure function, and variation of the excess entropy of mixing for the various families of compounds. We conclude with a discussion of projected trends.

2. BACKGROUND ON ENTROPY OF MIXING

The thermodynamic models developed for predicting polymer solution properties can be classified into two categories: lattice and off-lattice (or van der Waals) approaches. In both approaches the behavior of the molecule is typically described as a sum of an athermal (combinatorial or entropic) term and a residual (enthalpic, attractive, or potential energy) contribution. The athermal contribution assumes zero attractive energy interactions between the molecules, meaning that only size and shape of the molecules play roles in this case.[8,19] The athermal contribution prevails at high temperature where the kinetic energy of the molecules is larger than any interaction energy between them. The term "athermal" is applicable to both lattice and off-lattice models when the contribution is independent of temperature. In lattice models, it is assumed that each molecule and/or a segment of a molecule occupy a cell in the lattice and their arrangement depends on the composition, size, and shape of the molecule. The athermal contribution is obtained from the number of arrangements that is statistically possible in the lattice. Therefore, this contribution is often referred to as the combinatorial term. In off-lattice models, the athermal contribution can be addressed by computing the free energy of hard core molecules with no attractive interactions. The translational volume of the molecules is obtained from the difference between the total volume of the system and the occupied volume of the molecules.

The definition for excess entropy of mixing is the deviation from ideal solution behavior, i.e., mixtures with no volume, entropy, or enthalpy changes upon mixing (zero excess volume, excess entropy, and excess enthalpy),

$$S^{xs} = \Delta S_{Mix} - S^{is} \tag{1}$$

where S^{is} is the ideal solution entropy defined as $S^{is} = -\sum_i x_i \ln x_i$. To clarify, a well-known expression for the athermal excess entropy is the Flory–Huggins expression, which may be inferred using either a lattice or off-lattice perspective

$$S^{xs} = -R \sum_{i=s,p} x_i \ln \frac{\varphi_i}{x_i} \tag{2}$$

where $\varphi_i = x_i v_i / \Sigma\, x_i v_i$.

The "residual" contribution, originates from intermolecular attractions in both lattice and off-lattice models. Therefore, this term is usually referred to as the attractive, residual, the potential energy term, and sometimes enthalpic contribution because the differences in interaction energy generate heat of mixing. This contribution is obtained effectively from the product of characteristic energy per contact and the number of contacts in the system of interest for both lattice and off-lattice methods.[8] The residual contribution has been studied relatively often, with both on-lattice and off-lattice methods, as well as with hard cores and soft cores.[20,21]

The combinatorial contribution is calculated without regard to the attractive interactions between molecules and therefore it assigns a stochastic arrangement to the molecules. Random configuration of the molecules would mean that the mixing expression for the attractive energy term is so that the composition everywhere in the solution is equal to the overall composition. However, in real systems the molecular interactions cannot be ignored. Hence, in some of the advanced lattice[4] and off-lattice[22] models, local composition theory is used to correct for the nonrandom combinatorial contributions.[8,19] There are several theories to calculate nonrandomness behavior but in this work we only focus on the Guggenheim quasichemical approach.[3,23]

To the best of our knowledge, modern off-lattice theories are predominantly variations of the Boublik, Mansoori, Carnahan, Starling, and Leland (BMCSL) model.[11,24] Chapman et al. made a notable extension in formulating an equation of state for statistical associating fluid theory (SAFT).[25] Additionally, we describe our methodology, the SPEADMD approach, in the following sections.

2.1. Lattice Theories. Various lattice theories including the Prigogine cell model (PCM),[26] Flory–Orwoll–Vrij (FOV),[27] perturbed hard chain (PHC),[28] Sanchez–Lacombe (SL),[29−31] Costas–Santuary(C&S),[32−34] Panayiotou–Vera (PV),[5] GCLF,[6] UNIFAC-FV,[4] and Simha–Somcynsky(S&S)[35] has been introduced for polymer solutions. In the following subsections we consider FH, SL, GCLF, and UNIFAC-FV as representative samples and to cover simple approaches like FH, more complicated methods like SL, and a group contribution universal technique such as GCLF. Other proposed theories are based on similar concepts and have similar accuracy.

2.1.1. Flory–Huggins Model. The Flory–Huggins (FH) model that has been proposed 70 years ago is the basis for more

dx.doi.org/10.1021/ma402593m | Macromolecules 2014, 47, 1514−1531

rigorous theories developed in polymer science. This model has two parts. The first term comprises the combinatorial contributions to the entropy of mixing that are obtained from the number of ways that one can arrange polymer and solvent molecules on lattice sites. The resulting expression for entropy of mixing per mol is

$$\Delta S_{mix} = -R \sum_i x_i \ln \varphi_i \tag{3}$$

Therefore,

$$S^{xs} = -R \sum_{i=s,p} x_i \ln \frac{\varphi_i}{x_i} \tag{4}$$

where $\varphi_i = x_i v_i / \Sigma\, x_i v_i$. Here the volume fraction of solvent is $\Phi_s = (x_s v_s)/(x_s v_s + x_p v_p) = (x_s)/(x_s + \mathcal{R} x_p)$ and volume fraction of polymer is $\Phi_p = (x_p v_p)/(x_s \vartheta_s + x_p v_p) = (\mathcal{R} x_p)/(x_s + \mathcal{R} x_p)$ and $\mathcal{R} = v_p/v_s$ is the molecular volume ratio of polymer and solvent. It is assumed that the volume fractions, rather than mole fractions determine the excess entropy of mixing for molecules of different size. The second term of the FH model includes enthalpy of mixing and/or excess enthalpy of mixing that can be easily explained by the one-constant term in volume fraction (rather than mole fraction as in the case of Margules[36] equation)

$$\Delta H_{mix} = H^{xs} = \chi RT(x_s + m x_p)\varphi_s \varphi_p \tag{5}$$

where χ is the Flory parameter that depends only on interaction energies between molecules, i.e., residual contributions. This is consistent with the original definition[37−39] of solubility parameter (δ) which considers interaction energies and due to the regular solution theory (solutions that have zero excess volume and excess entropy changes, but a nonzero excess enthalpy). Nevertheless, both χ and δ parameters contain entropic contributions in addition to enthalpic contributions. Blanks and Prausnitz[39] (B&P) assumed the following relationship for mixing excess entropy of polymer solutions

$$\frac{-S_{0_{B\&P}}^{xs}}{R} = \sum_{i=s,p} x_i \ln \frac{\Phi_i}{x_i} + \chi^S \Phi_i \Phi_j (x_i + \mathcal{R} x_j) \tag{6}$$

where χ^S is the entropic Flory parameter. The Flory parameter, χ, can be calculated from,

$$\chi = \chi^H + \chi^S \tag{7}$$

where χ^H is the enthalpic term defined by Scatchard and Hildebrand as

$$\chi^H = \frac{\vartheta_s}{RT}(\delta_s - \delta_p)^2 \tag{8}$$

The entropic part $\chi^S = 1/z$, where z is the coordination number of the lattice, i.e., the number of sites that are nearest neighbors to a central site in the lattice. Blanks and Prausnitz[39] and Small[40] suggested that χ^S has a value between 0.3 to 0.4 for best results. These definitions and previous observations[8] convey an impression that such models are qualitative whereas we seek quantitative results.[41,42] The entropic effects are more important in polymer solution thermodynamics than small molecular systems. In polymer solutions entropic effects have stronger impacts on excess Gibbs energy and activity coefficient whereas in small molecular systems the enthalpic effects are the dominant factors. Another pitfall of the FH model is giving a single value of excess entropy, disregarding the change in packing fraction. A lattice hole theory would be needed to address changes in packing fraction. Also, this lattice model does not consider volume changes upon mixing of polymers and solvents which are also important in polymer melts.[43] These shortcomings make the model pressure independent and only applicable to liquids.

Flory[44] showed that the excess internal energy in FH theory is identical to that in the Scatchard−Hildebrand (SH) approach. The internal energy of the SH theory has been derived from the van der Waals equation (vdW) and hence the only difference between FH and vdW theories pertains to the excess entropy term. At some conditions a lattice theory like FH can be identical to an off-lattice model such as vdW, for both entropic and enthalpic terms. This unification happens when packing fraction is constant, regardless of composition and temperature, and for liquid states of matter where pressure influences are small.

2.1.2. Sanchez−Lacombe Equation of State. The Sanchez−Lacombe (SL) model[29−31] is based on the hole theory of Simha et al.[35] and uses a random mixing expression (no local composition effects) for the attractive energy term. This theory is very similar to FH theory except the packing fraction of the mixture varies by increasing the fraction of empty sites (holes) in the lattice. In this way, volume changes upon mixing are taken into account. In the FH approach all lattice sites are occupied by polymer segments and solvent molecules. The excess entropy of mixing for the SL EOS can be written as

$$-\frac{S^{xs}}{R} = \sum_i x_i \ln \frac{\varphi_i}{x_i} + r(\tilde{v} - 1)\ln(1 - \tilde{\rho}) + \ln \tilde{\rho} - \sum_i x_i [r_1^0 (\tilde{v}_i - 1)\ln(1 - \tilde{\rho}_i) + \ln \tilde{\rho}_i] \tag{9}$$

where $\tilde{\rho}$ is the reduced density, $r = \sum_i x_i r_i$, is the number of occupied lattice sites by polymer and solvent molecules, $\tilde{v} \equiv 1/\tilde{\rho} \equiv V/V^*$ is the reduced volume, $V^* = Nrv^*$, v^* is the close packed volume of a segment that comprises the molecules. Eq 9 reduces to FH when $\tilde{\rho} = \tilde{\rho}_i$ for the excess entropy of mixing. S^{xs} is athermal in the SL theory.

2.1.3. GCLF EOS. Group contribution lattice fluid theory (GCLF)[8] is a modified version of the Panayioutou−Vera[5] and SL[29−31] equations of state that has been recently extended to multicomponent systems.[6,45,46] The athermal excess entropy of mixing for this theory can be written as

$$-\frac{S^{xs}}{R} = \sum_i x_i \left[\ln \varphi_i - \ln w_i + \ln \frac{\tilde{v}_i}{\tilde{v}} + q_i \ln\left(\frac{\tilde{v}}{\tilde{v} - 1} \frac{\tilde{v}_i - 1}{\tilde{v}_i} \right) + \ln\left(M_i \sum_j \frac{w_j}{M_j} \right) \right] \tag{10}$$

where w_i, q_i, z_i, and M_i are the weight fractions, volume fractions, interaction surface area parameters, coordination number (usually set to 10), and molecular weights of component i in the mixture, respectively. S^{xs} varies with packing fraction in GCLF theory (like SL theory).

2.1.4. The Guggenheim−Stavermann Combinatorial Term (UNIFAC-FV). Oishi and Prausnitz[4] incorporated free volume differences between polymer and solvent contributions using the Guggenheim−Stavermann (GS) combinatorial term. For the residual term they have used Guggenheim's quasichemical theory. The free volume differences between polymer and

dx.doi.org/10.1021/ma402593m | Macromolecules 2014, 47, 1514−1531

solvent are not significant for small molecules but are extremely important for polymer solutions. The excess entropy of mixing for the GS model is also athermal

$$\frac{-S0_{GS}^{xs}}{R} = \sum_i x_i \ln \frac{\Phi_i}{x_i} - \frac{z}{2}\sum_j q_j x_j \ln\left(\frac{\Theta_j}{\Phi_j}\right) - \frac{S_{FV}^{xs}}{R} \quad (11)$$

where, $\Phi_j = (x_j q_j)/(\sum_j x_j q_j)$ and $\Theta_j = (x_j r_j)/(\sum_j x_j r_j)$ are the molecular volume fractions and surface fractions in the Guggenheim form of the excess entropy, respectively. Also $r_j = \sum_k \upsilon_k^{(j)} R_k$ and $q_j = \sum_k \upsilon_k^{(j)} Q_k$, where $\upsilon^{(j)}{}_k$ is the number of group of the k^{th} type in the j^{th} molecule. Also, R_k and Q_k are group contributions to the molecular parameters r_j and q_j. S_{FV}^{xs} is the free volume excess entropy of mixing given by the following equation

$$-\frac{S_{FV}^{xs}}{R} = \sum_{i=solvents} x_i \left\{ 3c_i \ln\left[\frac{\tilde{v}_i^{1/3} - 1}{\tilde{v}_M{}^{1/3} - 1}\right] - c_i\left[\left(\frac{\tilde{v}_i}{\tilde{v}_M} - 1\right)\left(\frac{1}{1 - \tilde{v}_i^{1/3}}\right)\right] + \ln\left(M_i \sum_j \frac{w_j}{M_j}\right)\right\} \quad (12)$$

In Eq12, c_i is an external degree of freedom parameter for solvent (usually 1.1), $\tilde{v}_i = (v_i M_i)/(0.01517 b r_i)$ is the reduced volume of solvent i, $\tilde{v}_M = (\sum_i v_i w_i)/(0.01517 b \sum_i (r_i w_i)/(M_i))$ is the reduced volume of mixture (v_i is the specific volume of solvent i [=] cm^3/g and b is the proportionality factor that is set to 1.28).

According to Danner and High,[8] the GS methodology cannot strictly be categorized as a lattice model, however. Although the combinatorial and residual parts are based on lattice theory, the free volume contribution has been derived from the Flory equation of state which is basically an off-lattice model. It has been suggested[8] that the combinatorial part of the GS theory exaggerates the nonideality in polymer solutions where the size and shape effects are important.

2.2. The SAFT Model as Representative of Off-Lattice Theories. Many off-lattice theories have been proposed during the past 70 years. Examples include works by Flory,[47] SAFT,[25] and Chen–Fredenslund–Rasmussen.[47] In the following subsections, we only discuss a tangent hard sphere model, i.e., SAFT equation of state.

The SAFT[25] model has been designed to describe the scaling with molecular weight of chain related terms in the equation of state. Therefore, chain properties should scale directly with the molecular weight (chain length or degree of polymerization (d_p) or carbon number (n_C)) in the long chain limit.

For SAFT theory[48] the excess entropy of mixing can be written as

$$-\frac{S^{xs}}{R} = \bar{m}\frac{A^{HS}}{N_s RT} - \sum_i x_i (m_i - 1) \ln g_{ii}^{hs}(\sigma_{ii}) \quad (13)$$

where $\bar{m} = \sum_i x_i m_i$ is the mean segment number in the mixture. The mixture version of the Helmholtz free energy of the hard-sphere fluid is defined on a per-segment basis as follows

$$\frac{A^{HS}}{N_S RT} = \frac{1}{\zeta_0}\left[\frac{3\zeta_1\zeta_2}{1 - \zeta_3} + \frac{\zeta_2{}^3}{\zeta_3(1 - \zeta_3)^2} + \left(\frac{\zeta_2{}^3}{\zeta_3{}^2} - \zeta_0\right)\ln(1 - \zeta_3)\right] \quad (14)$$

where N_S is the number of segments and the radial distribution function (RDF) of the hard-sphere fluid is given by

$$g_{ij}^{HS} = \frac{1}{1 - \zeta_3} + \left(\frac{3 d_i d_j}{d_i + d_j}\right)\frac{\zeta_2}{(1 - \zeta_3)^2} + \left(\frac{d_i d_j}{d_i + d_j}\right)^2 \frac{2\zeta_2{}^2}{(1 - \zeta_3)^2} \quad (15)$$

where $\zeta_n = \pi/6(\rho \sum_i x_i m_i d_i^n)$ and the temperature-dependent segment diameter d_i of compound i is

$$d_i = \sigma_i\left[1 - 0.12 \exp\left(-3\frac{\varepsilon_i}{RT}\right)\right] \quad (16)$$

Under athermal conditions (infinite temperature limit), eq 16 reduces to $d_i = 0.88\sigma_i$.

Finally, notice that both ESD[49] and s-SAFT[50−52] theories give a zero value for the excess entropy. For comparison, we present here a modification to s-SAFT (Ms-SAFT) that can reproduce good results for mixing excess entropy by defining the shape factor as

$$m^{s-SAFT} = m^{xs} + m^{sim} \quad (17)$$

$$m^{xs} = \Phi_{solvent}\Phi_{polymer} V_{mix}(1 - m_{ij})/V_{solvent} \quad (18)$$

where, $V_{mix} = \sum_i x_i V_i$ is the ideal mixing volume, m_{ij} is an adjustable binary parameter. The relationships for mixing excess entropy (repulsive mixing Helmholtz energy) of PC-SAFT and s-SAFT EOSs are available in the literature.[48−53]

3. METHODOLOGY

Molecular simulations of each reference fluid lead to a complete equation of state (EOS) specific to that particular molecular structure. For the implementation of DMD in the present work, we interpolate between simulated state points with a general EOS form that has proved capable interpolating quantitatively. We refer to this general EOS form as the SPEADMD EOS (step potentials for equilibria and discontinuous molecular dynamics).[54] We outline below our specific set of equations for deriving the properties of interest from simulation and performing the interpolations.

The SPEADMD approach consists of DMD simulations applied to calculate the repulsive fluid properties. The key data from the repulsive simulations are the compressibility factor, the site–site distance distributions, and their fluctuations. The virial theorem of Clausius gives the compressibility factor from the molecular simulation, comprising a summation of impacts over all collisions. The site–site distributions and fluctuations provide information which can be used to infer the behavior of the fluid with attractive intermolecular potentials at all temperatures.[55] The only quantity of interest for athermal S^{xs} calculations is the compressibility factor of the reference fluid. The site–site distributions and their fluctuations are ignored in the discussion below.

DMD simulation offers three key advantages for analyzing the excess athermal entropy. First, the sum of the virial (and the

dx.doi.org/10.1021/ma402593m | Macromolecules 2014, 47, 1514−1531

energy) is precise to machine precision (~12 significant figures), leading to precise values of the pressure at any given state point. For comparison, the conservation of energy in MD with a continuous potential is typically 4−6 significant figures. Second, the clear identification of a hard core reference potential eliminates ambiguity about the athermal limit. A soft reference potential, like the Lennard-Jones potential, would lead to results that vary with temperature. Third, the free energy (hence the entropy) is obtained by integration of the pressure with respect to density, minimizing the impact of any possible imprecision. Alternative approaches are more related to differentiation of the potential energy with particle insertion or deletion,[56] with consequent sensitivity to imprecision. Since the excess entropy is frequently a small difference between large numbers (i.e., the mixture entropy and the ideal solution value), its evaluation is particularly sensitive to any imprecision.

3.1. Simulation. Unlu et al.[54] developed a transferable potential model of alkane chains using butane, hexane, and hexadecane as training compounds and the lower *n*-alkanes through dodecane for validation. The basis of the model is to break the nonbonded potential function into four steps of variable well depth steps at $r/\sigma_{ij} = \{1.2, 1.5, 1.8, 2.0\}$ where σ_{ij} is the diameter of the *ij* interaction. For purposes of computing S^{xs}, the potential model of interest reduces to a single step from infinite energy to zero. It is valuable to note, however, that the site diameters of all molecules simulated in this work have been developed to transferably characterize the liquid density and vapor pressure of over 500 compounds with accuracy of 3% and 10% respectively over the entire range of available experimental data. This means that the sizes and shapes of the various molecular structures in this study bear a fairly accurate resemblance to the actual molecules themselves, in our opinion.

The simulations are performed with vibrating purely repulsive structures representative of united atom molecular models. For example, an explicit atom model of $-CH_2-$ would treat this functionality as three sites, while a united atom model treats it as a single spherical site. The bond lengths are constrained to be near the known values, e.g., 0.154 nm for a C−C single bond. Branches and rings are included directly according to the molecular structure. The bonded interactions are defined by

$$u_{ij}^{bonded} = \begin{cases} \infty & r < L_{12} - \delta_{12} \\ 0 & L_{12} - \delta_{12} \le r < L_{12} + \delta_{12} \\ \infty & L_{12} + \delta_{12} \le r < L_{13} - \delta_{13} \\ 0 & L_{13} - \delta_{13} \le r < L_{12} + \delta_{12} \\ \infty & L_{13} + \delta_{13} \le r < \sigma_{\text{int } ra} \\ 0 & \sigma_{\text{int } ra} \le r \end{cases}$$

$$u_{ij}^{non-bonded} = \begin{cases} \infty & r < \sigma \\ -\varepsilon_1 & \sigma \le r < 1.2\sigma \\ -\varepsilon_2 & 1.2\sigma \le r < 1.5\sigma \\ -\varepsilon_3 & 1.5\sigma \le r < 1.8\sigma \\ -\varepsilon_4 & 1.8\sigma \le r < 2.0\sigma \\ 0 & r \ge 2.0\sigma \end{cases} \quad (19)$$

The bonded interactions apply to intramolecular sites that are seven or fewer bonds apart. The nonbonded interactions in this work are the same for intermolecular interactions or intramolecular interactions more than seven bonds apart. Values of L_{12} and L_{13} are determined by average MNDO optimizations of the bond lengths and conformations for several typical compounds of the given functionality. Generally, $\delta_{ij} = 0.05L_{ij}$. Values of L_{12}, L_{13}, and σ_{intra} are available from previous SPEADMD publications and can be obtained by contacting the corresponding author. The details of nonbonded and bonded interactions of the step potentials are given in previous articles.[57]

The simulations were performed at packing fractions ranging from 0.1 to 0.5 ($\eta \in [0.1, 0.2, 0.3, 0.35, 0.4, 0.45, 0.5]$) and volume fractions of roughly 0, 0.1, 0.3, 0.5, 0.7, 0.9, and 1 at each packing fraction. Several types of mixtures were considered. The specific hydrocarbons studied were spherically shaped molecules represented as methane; linear molecules like ethane, *n*-butane, *n*-hexane, *n*-decane, and 1,3-butadiene; branched hydrocarbons such as isoprene, *trans*-2-butene, *cis*-2-butene, and 2,4-dimethylhexane (DMH); and ring aromatics such as toluene. A number of nonhydrocarbons were simulated such as: acetonitrile (ACN), heptafluoropropane (HFC-227ea), acetone (DMF), *n*-butylamine (C_4Amine), 3-pentylamine ($3C_5$Amine), and alcohols. The specific alcohols were water, ethanol, *n*-propanol, *n*-butanol, *n*-octanol, and 3-methylpentanol ($3MeC_5OH$). The polymer solutions were mixtures of a spherical molecule (methane), linear gas (ethane), branched hydrocarbon (DMH), or aromatic (toluene) with polyethylene or atactic random oriented styrenes, propylenes, or isoprenes with carbon numbers varying from 8 to 81.

For initialization, 100 copies of the prototype molecules were randomly inserted into the simulation box at each desired packing fraction. The infinite repulsions were converted temporarily to finite shoulders to permit brief molecular dynamics simulations of 10−200 fs with overlaps until the overlaps were eliminated. Connectivity indices were applied to maintain the integrity of the chain during this deoverlapping process. As overlaps were removed, the temperature was reset periodically by velocity rescaling. After a period of 10−100 short dynamic simulations in this manner, all overlaps were removed, providing unbiased, random initial configurations for the simulations. After initialization, each individual state point was simulated for 10 ns with 100 molecules for each specified packing fraction. Since only the trend in the repulsive term is concerned in this work, we neglect the effects of hydrogen bonding and attractive dispersion forces.

Characterizing the packing fraction requires accurate characterization of the effective volume, v^{eff}, of each molecule in the simulation. Each molecule can assume many conformations over the course of the simulations and the effective volume is the average over all conformations for a given molecule throughout a given simulation. Every 10 ps, 10 conformers are chosen at random for each molecule being simulated. The volumes are computed by a grid algorithm with a mesh of 0.01 nm.[54] Typically, v^{eff} varies weakly as a function of density and composition, making it possible to estimate its value a priori from simulation to simulation.

3.2. Interpreting Simulation Results. Simulation results must be manipulated to provide estimates of the excess entropy. The compressibility factor by itself is closely related to the athermal entropy but requires integration. Upon simulation at several densities and compositions, the computed entropy of the mixture must be rearranged to formulate the excess entropy. These manipulations are discussed below.

3.2.1. The Pure Fluid Contribution. The SPEADMD EOS is written in terms of the Helmholtz energy characterized by molecular simulation of the repulsive fluid (A_0). The thermodynamics of numerous molecular structures and chain lengths have been characterized with an interpolation formula that includes a hard sphere term, a chain term, and an effective number of tangent sphere segments in the chain, m.[58,59] The result is an equation of the form:

$$\left(\frac{A0(\eta, \vec{x}) - A^{id}}{RT}\right)_{T,V} = \left(\frac{A^{\circ} - A^{id}}{RT}\right)_{T,V} + (m-1)A0^{C} \tag{20}$$

where A is the molar Helmholtz energy, A° is the Helmholtz energy of the $m = 1$ reference system at the same packing fraction, and $A0^{C}$ refers to the reference term of the chain contribution. The relation between Helmholtz energy and compressibility factor is obtained through

$$\left(\frac{A0(\eta, \vec{x}) - A^{ig}}{RT}\right)_{T,V} = \int_0^{\eta} \frac{(Z0-1)}{\eta}\, d\eta \tag{21}$$

The subscript T,V in eq 21 emphasizes that this Helmoltz energy is to be evaluated with respect to a constant volume ideal gas reference state. Note that $A0/RT = U0/RT - S0/R$ and $U0 = 0$ for the reference fluid, where $U0$ and $S0$ refer to athermal internal energy and entropy, respectively. Hence the simulation of the reference fluid results in a precise measurement of the athermal entropy without any assumption of lattice behavior or neglect of branching or ring formation. We believe this method to provide precise estimates of S^{xs}.

Elliott and Gray,[60] showed the asymptotic behavior of the reference Helmholtz energy of pure *n*-alkanes based on SAFT and SPEADMD models. These two models have two major differences: (1) the SPEAD model implements a different reference fluid for each molecular geometry, whereas the SAFT model uses a tangent-spherical reference fluid for all molecules (2) the SPEADMD model is formulated at the level of transferable characterizations of interaction sites whereas the SAFT model is formulated at the molecular level. The general formula for reference compressibility factor of SAFT and SPEADMD is[60]

$$Z0^{SAFT} = 1 + m(Z^{HS} - 1) - (m-1)\frac{\eta(5-2\eta)}{(1-\eta)(2-\eta)} \tag{22}$$

$$Z0^{SPEADMD} = 1 + m(Z^{HS} - 1) - (m-1)\frac{\eta(6\eta^2 - 6\eta + 1)}{(1-\eta)^3}\left[1 + \kappa\frac{m-1}{m}\right] \tag{23}$$

where $Z^{HS} = (1 + \eta + \eta^2 - \eta^3)/(1-\eta)^3$ is the hard sphere compressibility factor, and κ and m are given in our previous work[59] for various polymers. In both models, the m parameter is used to characterize the shape of the molecule. In SAFT, this parameter is fit to experimental data with $(m-1) = m_0(N_C - 1)$, while including effects of the attractive contribution. In SPEADMD, the m parameter (along with the κ parameter) is fit to simulation data of the reference fluid with $m - 1 = m_0(N_C - 1) + m_1(N_C - 1)^2/N_C$.[58,60] The values of m_0, m_1 are given in the Vahid and Elliott paper[59] for various molecular structures and for each equation of state.

It should be noted that Rosenfeld et al.[15,16,61] use the term "excess entropy" for what we call the entropy departure function of a pure fluid: $-(S - S^{ig})/R$.

$$\begin{aligned} -(S - S^{ig})/R &= (A - A^{ig})/RT - (U - U^{ig})/RT \\ &= A0 + A_1/T + A2/T^2 - (A1/T + 2A2/T^2) \\ &= A0 - A2/T^2 \end{aligned} \tag{24}$$

where the ig refers to ideal gas condition. The quantities $A0$, $A1$, and $A2$ in eq 24 are temperature independent expansion coefficients, and the equation is only accurate to second order in temperature. These quantities should not be confused. Our manuscript deals only with the athermal entropy departure and its mixing, as given by the $A0$ term in eq 24 through integration of eq 21

3.2.2. Mixtures. Gray and Elliott[12] provided a preliminary analysis to obtain the best interpolation rule for our simulations. They suggested the following equation

$$A0 = \frac{\sum_i \sum_j x_i x_j A0_{ij} (b_i b_j)^{1/2}}{\sum_i x_i b_i} \tag{25}$$

In eq 25, x_i is the mole fraction of the ith component, and b_i is the molar volume of the ith molecule. $A0_{ii}$ is the pure fluid repulsion Helmholtz energy and $A0_{ij} = (A0_{ii}\, A0_{jj})^{1/2}\,(1 - k_{ij}^{S})$ is the cross repulsive Helmholtz energy. We would like to characterize the trends for $A0$ such that the equation of state can be computed in the usual fashion to obtain activities and PVT properties. We have considered several candidates for performing this interpolation function. We refer to the simplest as van der Waals mixing. Eq 25 can be rearranged to,

$$\frac{A0^{xs}_{vdW}}{RT} = \frac{-S0^{xs}_{vdW}}{R} = \frac{\langle b \rangle}{R} \sum_{ij} \Phi_i \Phi_j \chi_{ij}^{S} \tag{26}$$

where $\langle b \rangle = \sum_i x_i b_i$ is the molar average molecular volume, $b_i = N_A v_i^{eff}$ is the molar volume, N_A is Avogadro's number, v_i^{eff} is the molecular effective volume, $\Phi_i = x_i v_i^{eff}/\sum_i x_i v_i^{eff}$ is the volume fraction, $\eta = b\rho$ is the packing fraction, and ρ is the molar density. Note that the excess properties are typically defined as the system deviation from the ideal solution behavior at the same temperature, pressure, and mole fraction. However, the definition proposed in this work is based on Helmholtz free energy, i.e., is based on the difference between the property of the system and that of an ideal solution at the same temperature, packing fraction, and mole fraction. The ideal solution is defined as the mole fraction based sum of the mixture athermal entropy as

$$S^{is} = \sum_i x_i S0_i \tag{27}$$

$$\chi_{ij}^{S}(\eta) = \frac{2S0_{ij}}{(b_i b_j)^{1/2}} - \left(\frac{S0_{ii}}{b_i} + \frac{S0_{jj}}{b_j}\right) \tag{28}$$

$$S0_{ij} = (S0_i \times S0_j)^{1/2}(1 - k_{ij}^{S}) \tag{29}$$

where k_{ij}^{S} is the entropic binary interaction parameter.

Rearranging shows that, at $\eta = 0.4$

$$\begin{aligned} \chi_{ij}^{S} &= -[(\delta_j^S)^2 - 2\delta_i^S\delta_j^S(1 - k_{ij}^{S}) + (\delta_i^S)^2] \\ &= -(\delta_j^S - \delta_i^S)^2 - 2(\delta_i^S\delta_j^S)k_{ij}^{S} \end{aligned} \tag{30}$$

dx.doi.org/10.1021/ma402593m | Macromolecules 2014, 47, 1514−1531

where

$$\delta_i^S \equiv [(A0_{ii}|_{\eta=0.4})/b_i]^{1/2}\ [\ =\ ]\ (\mathrm{cal/cm^3})^{1/2} \tag{31}$$

is defined as the entropic (athermal) solubility parameter. Eq 30 is used to evaluate k_{ij}^S from simulation results at $\eta = 0.4$. The value of $\eta = 0.4$ is chosen as an arbitrary reference condition that is representative of the middle of the liquid range. The traditional standard for solubility parameter is defined in terms of the "liquid" at 298 K. We prefer to avoid the ambiguity that arises for gaseous components when defining a new reference condition by specifying the packing fraction instead of the "liquid" state. We maintain the application of 298 K as an indicator of thermal energy, however, in order to maintain the scale of magnitude that is familiar with Hildebrand solubility parameters. Recently,[62,63] a study has been performed on a PIP−PS polymer blend to test the applicability of the empirical mixing rules. It has been stated that the empirical mixing rule (Lorentz−Berthelot) underestimates the phase separation tendency and hence leads to a mixed system which is in disagreement with available experimental data.[64] However, they apparently confused the term mixing rule with combining rule and so the reliability of the vdW mixing rules was not at issue.

Note that χ^S is a function of packing fraction, because $A0_{ii}$ and k_{ij}^S are functions of η ($k_{ij}^S = k_{ij}^{S0} + \eta k_{ij}^{S1}$). In the discussion below, we consider several prospective approximations to k_{ij}^S and compare them with results of the simulations. If we ignore the density dependence of k_{ij}^S, i.e., $k_{ij}^{S1} = 0$, an extremely useful approximation would be $k_{ij}^{S0} \sim -0.04\chi_0^S$, where $\chi_0^S = (b_i + b_j)/600R(\delta_s^S - \delta_p^S)^2$ for the whole database. For polymer mixtures we observed improved predictions of phase behavior with the correlation,

$$k_{ij}^{S0} = \frac{-0.04 \times 18 \times (n_p + n_s) \times \chi_0^S}{\sum_i v^{\mathrm{eff}}} \tag{32}$$

where n_p and n_s are the numbers of polymer and solvents in the system, respectively. This approximation approaches $k_{ij}^{S0} \sim -0.04\chi_0^S$ for mixtures of small molecules (where $v_i^{\mathrm{eff}} \sim 18\ \mathrm{cm^3/mol}$) and it approaches zero when large molecules are included in the mixture. Notice that with this default approximation, simulation of the mixture to determine the entropy of mixing becomes unnecessary. We will show that this universal approximation provides near quantitative accuracy for all mixtures studied, including aromatic, aliphatic, and alcohol mixtures with volume ratios ($\mathcal{R}$) approaching ∞:1. To appreciate how this is possible, one must recognize that *S*0 is purely repulsive. Therefore, contributions to *S*0 are simply related to effects of size and shape. By accounting for the entropy density through the entropic solubility parameter, a universal rule for k_{ij}^{S0} becomes feasible. For truly quantitative representations of simulation data, $k_{ij}^{S1} \neq 0$ and the optimal values of k_{ij}^{S0} and k_{ij}^{S1} must be characterized from simulation data. The optimization procedure has been performed using the Levenberg−Marquardt algorithm based on MINPACK[65] routines.

4. RESULTING TRENDS

Before analyzing the trends for mixtures, it is valuable to consider the trend in entropic solubility parameter vs molecular weight. The entropy density exhibits trends that may seem counterintuitive at first. This sets the stage for the follow-up analysis of mixtures.

4.1. Trends in the Entropic Solubility Parameter. The entropic solubility parameter, as defined by eq 31, exhibits systematic trends with molecular structure and density. Figure 1 shows the values for the entropic solubility parameter of various molecular structures as they approach the long chain limit. Briefly, the entropy density of a small molecule is much higher than that of large molecule in the nature of its impact on the excess entropy. This implies that the excess entropy is inherently smaller when only large molecules are mixed. It should be noted, however, that small magnitudes of excess entropy can strongly affect the estimated entropic activity of large molecules because the activity (a derivative property) multiplies the nonideality by the volume the molecule, which can be quite large. Therefore, this trend in entropy density may seem counterintuitive at first, but must be born in mind when considering the behavior of mixtures.

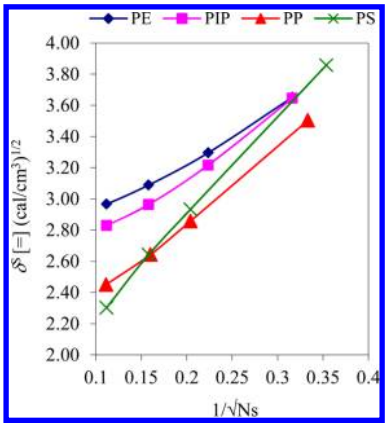

Figure 1. Asymptotic trends for the entropic solubility parameter of various polymer structures in the infinite chain limit. *Ns* is the number of the molecular sites in the polymer chain.

Figure 1 also shows that polyethylene (PE), polyisoprene (PIP), and polypropylene (PP) generate similar asymptotes in entropic solubility parameter but the polystyrene (PS) asymptote is different. This may be attributable to the presence of the rings in the macromolecule structure. Eq 30 indicates that the difference in solubility parameter has the primary effect. Therefore, this difference will be largest when long aromatic chains are mixed with small molecules. The difference may be smallest, however, when small aromatic molecules are mixed with small molecules, owing to the steeper slope for aromatic chains. Without understanding the distinctive trend for aromatic chains in Figure 1, it might seem surprising for aromatic molecules to change their behavior so much when only the molecular weight is varied.

4.2. Trends in Athermal Excess Entropy. The various theories should be tested through extensive off-lattice molecular simulation using transferable potential models that have proved reliable for the properties of linear, branched, cyclic and aromatic molecules.[13,54,66−69] In particular, we would like to address key questions about the applicable range of eqs 26−30. For example, are these equations valid for long chains? If so, how long must the chain be for the asymptotic equations to provide an accurate representation? Are they equally valid for branched, cyclic, and aromatic molecules? What is the detailed variation of each term with density and chain length? This subsection presents a detailed evaluation of the vdW mixing rule and analysis of the excess entropy of the polymer solutions.

Inferring the general trends with composition and density requires simulations at many state points. Figure 2 illustrates

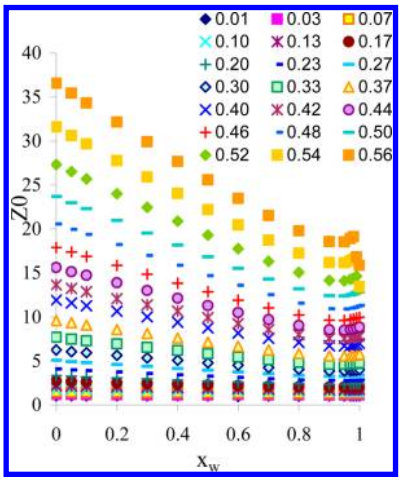

Figure 2. Reference fluid compressibility factor for the octanol + water system. x_w represents the mole fraction of water. Packing fractions are listed in the legend, illustrating the range of coverage and of state points simulated.

the coverage of the composition and density for the reference fluid simulations. In all, 294 state points were simulated for this one binary mixture, not including the 42 state points simulated for the pure components. While this may seem like a large number of simulations, it is small compared to what would be required if temperature were to be varied with a similar degree of resolution, as would be required for simulations of soft potential models. The adoption of the discontinuous potential permits this reduction in state space, facilitating the systematic analysis of trends. We discuss the details of the reference term contribution below, which establishes the basis for analyzing the other contributions (first and second).

The $Z0$ quantity is a direct result of summing the virial, hence it is not subject to the approximations of perturbation theory. Note that the results for pure "water" exhibit a sharp drop at packing fractions greater than 0.5. "Water" in this case refers simply to a hard sphere with a diameter of 0.3 nm, because the reference system does not include the disperse attractions or hydrogen bonding interactions. Hence the sharp drop is a consequence of crystallization in the hard sphere fluid, for which the maximum stable liquid packing fraction is 0.494. The results for pure water are therefore metastable at packing fractions of 0.5−0.52. The trend at $x_{C8} = 0.02$ indicates that the octanol disrupts the water crystallization at this mole fraction (and a volume fraction of 0.15). This crystallization is only an issue for binary systems involving water or methane. The trends for all other systems exhibit stable liquid behavior for all packing fractions.

The trends in Figure 2 suggest that the mixing behavior should be analyzed in terms of the excess behavior, to amplify the deviations from ideality at low packing fractions. Furthermore, the trend is skewed toward the smaller component. Placing the compositions on a volume fraction basis helps to adjust for the skewness. Therefore, we consider the excess functions in terms of volume fractions in subsequent discussion. Finally, we recognize that the Helmholtz energy of the reference system is simply related to the entropy, through eq 24, and label the ordinate accordingly. Thus, integrating the state points in Figure 2 at constant composition yields the entropy departure function. This leads to Figure 3 for the entropy departure function of the athermal system. The points

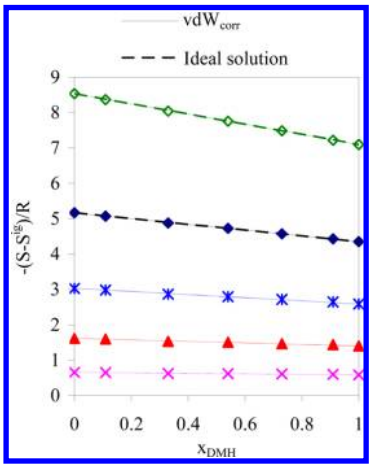

Figure 3. Entropy departure function for DMH + PIP (C_{10}) based on vdW MR with $\mathcal{R} = 1.16$ and $\delta_s^S/\delta_p^S = 1.12$ at packing fractions of 0.1 (pink), 0.2 (red), 0.3 (blue), 0.4 (dark blue), and 0.5 (green).

in the figure represent the simulation result and the solid curves are the interpolations based on eqs 26−30. We conclude that the van der Waals mixing model provides an accurate description of the simulation results for this mixture of a sphere with a chain.

In this research, two key parameters play roles in determining the nonideality: the volume ratio ($\mathcal{R}$ = the ratio of the effective volumes of the polymer to the solvent) and the ratio of the entropic solubility parameters of solvent and "polymer" (δ_s^S/δ_p^S). The impact of $\mathcal{R}$ has been recognized since the early work of Mansoori et al.[11] One hypothesis in this work was to consider mixtures with $\mathcal{R} < 2$ as ideal and the rest as nonideal. This hypothesis is not always true, however. To elaborate, we classify our polymer solutions and mixtures into three categories:

Our first category considers approximately ideal solutions, i.e., mixtures (of solvents) and polymer solutions where $\mathcal{R} < 2$ and $\delta_s^S/\delta_p^S < 1.5$ (usually mixtures with volume ratios close to one). In this case, the average absolute deviation (AAD) in the athermal excess entropy of mixing, i.e., $(S_{AAD}^{xs})/R = (|S_{calc}^{xs} - S_{sim}^{xs}|)/R$ is extremely small, e.g., ∼ 0.010 for vdW_0 (vdW mixing rule with $k_{ij}^{S0} = 0$), 0.008 for vdW_1 (vdW mixing rule with k_{ij}^{S0} treated as an adjustable parameter), 0.007 for vdW_2 (vdW mixing rule with two interaction parameters), and 0.009 for vdW_{corr} (vdW mixing rule with k_{ij}^{S0} of eq 32 according to Table 1. However, the ratio of the deviations to the absolute maximum simulated excess entropy, $(S_{AAD}^{xs})/(\text{Max}|S_{Sim}^{xs}|)$ is high, i.e., ∼36% for vdW_0, 28% for vdW_1, 24% for vdW_2, and 36% for vdW_{corr} because the excess entropy is almost zero for the mixtures and polymer solutions that belong to the first category. The physical interpretation is that the athermal excess entropy of mixing is extremely small for the first category. This observation is consistent with the works by Mathias and co-workers[70] and Gray et al.[12] Figure 3 and S1−S24 of the Supporting Information illustrate ideal solution behavior where the excess entropy is small.

The second category of polymer solutions are moderately nonideal solutions where $\mathcal{R} > 2$ but $\delta_s^S/\delta_p^S < 1.5$ (polymers with "good" solvents: small entropic solubility parameter difference, i.e., various molecular structures of polymers with

dx.doi.org/10.1021/ma402593m | Macromolecules 2014, 47, 1514−1531

Table 1. Summary of Simulation Data and Model Predictions for Different Mixture Volume Ratios of Polymer Solutions Based on the vdW Mixing Rule

							vdW$_0$		vdW$_1$		vdW$_2$		vdW$_{corr}$	
			$N_c^{\$}$	$\mathcal{R}$	δ_s^S/δ_p^S	max$\lvert S^{xs}_{Sim}\rvert$	S^{xs} AAD *	(S^{xs} AAD)/(max$\lvert S^{xs}_{Sim}\rvert$)	S^{xs} AAD	(S^{xs} AAD)/(max$\lvert S^{xs}_{Sim}\rvert$)	S^{xs} AAD	(S^{xs} AAD)/(max$\lvert S^{xs}_{Sim}\rvert$)	S^{xs} AAD	(S^{xs} AAD)/(max$\lvert S^{xs}_{Sim}\rvert$)
Polymer Solutions and Mixtures η = 0.5														
Nonideal														
1	octanol	water	8	9.84	2.42	0.975	0.079	0.081	0.019	0.020	0.013	0.014	0.021	0.022
2	methane	isoprene	5	3.21	1.59	0.305	0.013	0.043	0.007	0.025	0.004	0.012	0.007	0.025
3	PE	methane	10	6.06	1.89	0.568	0.023	0.040	0.014	0.024	0.005	0.009	0.016	0.029
4			20	11.62	2.10	0.790	0.054	0.068	0.029	0.037	0.011	0.014	0.040	0.050
5			40	22.53	2.24	1.073	0.067	0.063	0.049	0.046	0.006	0.006	0.053	0.049
6			80	44.53	2.33	1.327	0.105	0.078	0.067	0.050	0.014	0.010	0.052	0.069
7		ethane	10	3.86	1.53	0.255	0.018	0.072	0.009	0.035	0.004	0.015	0.009	0.036
8			16	5.98	1.65	0.380	0.034	0.090	0.015	0.040	0.004	0.011	0.015	0.040
9			20	7.38	1.70	0.447	0.038	0.085	0.018	0.040	0.004	0.009	0.017	0.053
10			40	14.40	1.81	0.627	0.055	0.087	0.028	0.045	0.009	0.014	0.040	0.064
11			80	27.97	1.91	0.606	0.085	0.140	0.042	0.069	0.007	0.012	0.067	0.110
12	PIP	methane	10	5.93	1.89	0.594	0.031	0.052	0.019	0.033	0.007	0.012	0.020	0.033
13			20	11.27	2.15	0.814	0.053	0.065	0.028	0.034	0.004	0.005	0.033	0.040
14			40	21.97	2.33	1.034	0.076	0.073	0.041	0.040	0.008	0.008	0.054	0.052
15			80	43.18	2.43	1.341	0.109	0.081	0.063	0.047	0.008	0.006	0.055	0.074
16		ethane	10	3.78	1.53	0.267	0.023	0.087	0.009	0.035	0.005	0.018	0.011	0.041
17			20	7.18	1.74	0.449	0.049	0.110	0.021	0.046	0.005	0.011	0.021	0.047
18			40	13.99	1.89	0.612	0.07	0.114	0.034	0.056	0.006	0.010	0.040	0.065
19			80	27.50	1.97	0.912	0.104	0.114	0.052	0.057	0.010	0.011	0.064	0.070
20	PP	methane	9	5.68	1.97	0.634	0.037	0.059	0.024	0.037	0.008	0.012	0.024	0.037
21			24	14.37	2.42	1.028	0.071	0.069	0.038	0.037	0.006	0.006	0.049	0.047
22			39	23.00	2.57	1.194	0.086	0.072	0.049	0.041	0.005	0.004	0.057	0.051
23			81	47.27	2.77	1.326	0.152	0.114	0.072	0.054	0.021	0.016	0.083	0.063
24		ethane	9	3.62	1.60	0.300	0.03	0.101	0.014	0.048	0.005	0.016	0.017	0.055
25			24	9.16	1.96	0.611	0.063	0.103	0.029	0.048	0.003	0.006	0.029	0.049
26			39	14.65	2.08	0.775	0.085	0.114	0.041	0.055	0.004	0.005	0.045	0.058
27			81	30.10	2.24	0.820	0.14	0.171	0.055	0.067	0.018	0.022	0.059	0.072
28	PS	methane	8	4.14	1.79	0.502	0.014	0.028	0.012	0.023	0.004	0.008	0.013	0.026
29			24	11.53	2.36	0.968	0.058	0.060	0.032	0.033	0.007	0.007	0.041	0.042
30			40	18.85	2.61	1.144	0.08	0.070	0.044	0.038	0.009	0.008	0.073	0.063
31			80	37.36	3.00	1.282	0.079	0.068	0.051	0.062	0.016	0.012	0.065	0.051
32		ethane	8	2.63	1.55	0.188	0.01	0.051	0.006	0.029	0.004	0.020	0.006	0.029
33			24	7.34	1.91	0.589	0.042	0.072	0.020	0.034	0.004	0.006	0.019	0.033
34			40	12.00	2.12	0.747	0.085	0.114	0.041	0.055	0.004	0.005	0.040	0.053
35			80	23.80	2.43	0.809	0.156	0.192	0.064	0.080	0.015	0.018	0.082	0.102
	total nonideal						**0.065**	**0.086**	**0.033**	**0.043**	**0.008**	**0.011**	**0.039**	**0.050**
Moderately Nonideal														
36	PE	toluene	20	3.23	1.22	0.085	0.01	0.121	0.009	0.102	0.006	0.074	0.009	0.103
37			40	6.21	1.29	0.155	0.029	0.185	0.021	0.136	0.011	0.068	0.021	0.136

dx.doi.org/10.1021/ma402593m | *Macromolecules* 2014, 47, 1514−1531

Table 1. continued

			$N_c^{\$}$	$\mathcal{R}$	δ_s^S/δ_p^S	max|S^{xs}_{Sim}|	vdW$_0$		vdW$_1$		vdW$_2$		vdW$_{corr}$	
							S^{xs} AAD *	(S^{xs} AAD)/(max|S^{xs}_{Sim}|)	S^{xs} AAD	(S^{xs} AAD)/(max|S^{xs}_{Sim}|)	S^{xs} AAD	(S^{xs} AAD)/(max|S^{xs}_{Sim}|)	S^{xs} AAD	(S^{xs} AAD)/(max|S^{xs}_{Sim}|)
Polymer Solutions and Mixtures η = 0.5														
Nonideal														
Moderately Nonideal														
38			80	12.30	1.38	0.161	0.057	0.352	0.022	0.136	0.013	0.079	0.022	0.137
39		DMH	20	2.26	1.09	0.057	0.009	0.164	0.005	0.095	0.005	0.087	0.009	0.164
40			40	4.35	1.18	0.123	0.010	0.081	0.009	0.075	0.008	0.069	0.010	0.081
41			80	8.61	1.24	0.223	0.041	0.185	0.021	0.094	0.017	0.074	0.023	0.102
42	PIP	toluene	20	3.14	1.25	0.148	0.022	0.149	0.011	0.074	0.007	0.047	0.013	0.087
43			40	6.12	1.34	0.184	0.034	0.185	0.015	0.082	0.009	0.049	0.023	0.125
44			80	12.02	1.39	0.199	0.052	0.261	0.021	0.106	0.013	0.065	0.031	0.154
45		DMH	20	2.20	1.12	0.047	0.006	0.125	0.006	0.124	0.006	0.119	0.006	0.126
46			40	4.28	1.21	0.109	0.016	0.148	0.011	0.099	0.007	0.066	0.013	0.115
47			80	8.41	1.26	0.212	0.028	0.133	0.028	0.130	0.014	0.064	0.028	0.131
48	PP	toluene	24	4.00	1.40	0.190	0.03	0.156	0.017	0.092	0.010	0.050	0.018	0.095
49			39	6.41	1.48	0.307	0.031	0.100	0.021	0.069	0.011	0.037	0.023	0.074
50			81	13.16	1.49	0.375	0.042	0.112	0.033	0.088	0.018	0.048	0.037	0.099
51		DMH	24	2.80	1.26	0.108	0.021	0.192	0.013	0.119	0.008	0.076	0.015	0.135
52			39	4.48	1.34	0.203	0.026	0.130	0.016	0.081	0.004	0.021	0.017	0.081
53			81	9.21	1.45	0.223	0.034	0.152	0.031	0.304	0.015	0.067	0.032	0.143
54	PS	toluene	24	3.21	1.36	0.155	0.016	0.101	0.010	0.066	0.009	0.058	0.011	0.068
55			40	5.25	1.48	0.288	0.045	0.157	0.023	0.079	0.003	0.009	0.023	0.081
56			80	10.40	1.49	0.258	0.059	0.229	0.029	0.112	0.016	0.062	0.033	0.128
57		DMH	24	2.25	1.22	0.055	0.032	0.575	0.019	0.339	0.012	0.218	0.028	0.512
58			40	3.67	1.35	0.130	0.049	0.373	0.021	0.164	0.015	0.118	0.034	0.264
59			80	7.23	1.49	0.144	0.056	0.389	0.028	0.194	0.017	0.118	0.037	0.257
	total moderately nonideal						**0.031**	**0.198**	**0.018**	**0.123**	**0.011**	**0.073**	**0.022**	**0.142**
Ideal														
60	PE	toluene	10	1.69	1.09	0.030	0.009	0.311	0.007	0.226	0.006	0.213	0.009	0.311
61		DMH	10	1.18	1.02	0.029	0.011	0.383	0.009	0.322	0.009	0.309	0.011	0.383
62	PIP	toluene	10	1.65	1.10	0.074	0.024	0.319	0.023	0.306	0.022	0.305	0.024	0.322
63		DMH	10	1.16	1.01	0.022	0.008	0.364	0.008	0.315	0.007	0.318	0.007	0.321
64	PP	toluene	9	1.58	1.14	0.033	0.011	0.338	0.010	0.317	0.009	0.283	0.011	0.324
65		DMH	9	1.11	1.03	0.021	0.014	0.635	0.009	0.419	0.005	0.218	0.014	0.632
66	PS	toluene	8	1.15	1.04	0.042	0.011	0.256	0.008	0.203	0.008	0.201	0.009	0.222
67		DMH	8	1.24	1.08	0.070	0.021	0.296	0.011	0.161	0.007	0.101	0.020	0.290
68	ACN	*trans*-2-butene	4	1.40	1.17	0.026	0.006	0.225	0.005	0.183	0.004	0.145	0.005	0.204
69		*cis*-2-butene	4	1.40	1.16	0.020	0.002	0.108	0.002	0.107	0.002	0.106	0.002	0.107
70		1,3-butadiene	4	1.28	1.13	0.014	0.004	0.312	0.003	0.229	0.002	0.184	0.004	0.285
71	ethanol	R227	3	1.77	1.20	0.067	0.006	0.090	0.006	0.085	0.006	0.083	0.006	0.087
72	DMF	*trans*-2-butene	4	1.06	1.00	0.015	0.006	0.417	0.004	0.291	0.003	0.193	0.006	0.417
73		*cis*-2-butene	4	1.06	1.05	0.022	0.003	0.116	0.003	0.115	0.002	0.114	0.003	0.116

dx.doi.org/10.1021/ma402593m | *Macromolecules* 2014, 47, 1514−1531

Table 1. continued

		N_c[§]	$\mathcal{R}$	δ_s^S/δ_p^S	max|S^{xs}_{Sim}|	vdW$_0$ S^{xs} AAD*	vdW$_0$ (S^{xs} AAD)/(max|S^{xs}_{Sim}|)	vdW$_1$ S^{xs} AAD	vdW$_1$ (S^{xs} AAD)/(max|S^{xs}_{Sim}|)	vdW$_2$ S^{xs} AAD	vdW$_2$ (S^{xs} AAD)/(max|S^{xs}_{Sim}|)	vdW$_{corr}$ S^{xs} AAD	vdW$_{corr}$ (S^{xs} AAD)/(max|S^{xs}_{Sim}|)
Polymer Solutions and Mixtures η = 0.5													
Nonideal													
74	1,3-butadiene	4	1.16	1.03	0.013	0.005	0.358	0.003	0.270	0.003	0.255	0.005	0.355
75	butane perfluoroC4	4	1.52	1.05	0.015	0.008	0.546	0.005	0.339	0.004	0.254	0.008	0.537
76	hexane butanol	6	1.32	1.11	0.027	0.014	0.500	0.013	0.467	0.012	0.452	0.014	0.500
77	C_4amine propanol	4	1.28	1.09	0.015	0.012	0.816	0.008	0.530	0.007	0.457	0.011	0.815
78	butanol	4	1.28	1.13	0.024	0.011	0.431	0.007	0.287	0.004	0.186	0.011	0.430
79	3-MeC$_5$OH	8	1.24	1.03	0.023	0.007	0.312	0.005	0.205	0.004	0.174	0.007	0.309
80	3C$_5$amine	8	1.40	1.06	0.017	0.008	0.485	0.005	0.284	0.004	0.234	0.008	0.468
81	hexane	8	1.34	1.07	0.033	0.013	0.414	0.013	0.407	0.013	0.399	0.013	0.402
	total ideal					**0.010**	**0.365**	**0.008**	**0.276**	**0.007**	**0.236**	**0.009**	**0.356**
	total					**0.040**	**0.195**	**0.022**	**0.130**	**0.008**	**0.090**	**0.026**	**0.160**

[§]N_c = number of carbons in polymer molecule (degree of polymerization × number of carbon in the repeating unit). *$S^{xs}_{AAD} = |S^{xs}_{calc} - S^{xs}_{sim}|$ calc = model prediction, sim = simulation data.

branched and/or ring solvents). In this case, the average absolute deviation of the athermal excess entropy of mixing, i.e., $(S^{xs}_{AAD})/R = (|S^{xs}_{calc} - S^{xs}_{sim}|)/R$ is ~0.031 for vdW$_0$, 0.018 for vdW$_1$, 0.011 for vdW$_2$, and 0.022 for vdW$_{corr}$ Note that in this condition, only the deviations for vdW$_2$ can be designated as quantitative because these mixtures and polymer solutions are in a transition state between ideal and nonideal solutions. The absolute maximum excess entropy for this category is smaller than the expected value for the mixtures with the same molecular volume ratio and $\delta_s^S/\delta_p^S > 1.5$ and is larger than mixtures with $\mathcal{R} < 2$ and $\delta_s^S/\delta_p^S < 1.5$. This means that both $\mathcal{R}$ and δ_s^S/δ_p^S have important roles in characterizing a solution's nonideality. On the other hand, branching and rings in the solvent moderate the nonideality. Comparing the effect of branching to the effect of rings, DMH indicates a more nonideal solution than toluene because it has a larger entropic solubility parameter (4 compare to 3.6 $(cal/cm^3)^{1/2}$). This means that the effect of δ_s^S/δ_p^S is more important than $\mathcal{R}$ in determining the nonideal behavior for these mixtures. Figures 4 (ring solvent), 5 and 6 (branched solvents) illustrate polymer solutions that belong to the second category.

The third category of mixtures and polymer solutions are those with $\mathcal{R} > 2$ and $\delta_s^S/\delta_p^S > 1.5$ (polymer solutions that solvents are either a spherical shape and/or a linear gas with no branching and ring effects and polymers are all various kinds of molecular structures). In these situations, the systems are highly nonideal. Figure 7 illustrates a typical example of such cases.

Owing to precision issues with these computations, we find it useful to tabulate a quantitative measure of the degree of scatter relative to the magnitude of the excess entropy. For this purpose, we characterize the magnitude of the excess entropy by its maximum absolute value. We find that the vdW$_2$ model provides a characterization that is within the range of scatter and therefore, the ratio of $(S^{xs}_{AAD})/(\text{Max}|S^{xs}_{Sim}|)$ for the vdW$_2$ model can be considered as a "noise to signal" ratio. When this ratio is large (e.g., 33% for ideal mixtures), it means that the magnitude of the nonideality is so small that measuring it becomes difficult. It would be misleading to summarize deviations in terms of the percent deviation for each point because the excess entropy approaches zero at either end of the composition range and dividing by such small numbers would amplify these deviations artificially. We also tabulate this ratio for the other models to facilitate comparisons and refer to it generally as the "percent deviation" although its definition differs from the usual definition of this term. For example, percent deviations in the nonideal category are: $(S^{xs}$ AAD)/$(\text{Max}|S^{xs}_{Sim}|)$~ 9% for vdW$_0$, 4% for vdW$_1$, 1% for vdW$_2$, and 5% for vdW$_{corr}$. These results indicate that any deviations greater than 1% indicate that the model is not quantitative, but deviations of 4−5% are still quite small. They also indicate that the 1-parameter fit of the vdW$_1$ model provides little improvement over the generalized correlation.

Figure 8 is a summary of these three classes of mixtures and polymer solutions in our study. Clearly, mixtures that have higher volume ratios do not necessarily have higher absolute maximum athermal excess entropy (Figure 8, parts a and 8b). A general plot would be the plot of maximum athermal excess entropy versus the ratio of the entropy density of a solvent and its polymer. As shown in Figure 8c, the maximum absolute excess entropy of mixing increases monotonically with δ_s^S/δ_p^S.

On the basis of these observations and the classifications of the polymer solutions and mixtures, $(S^{xs}_{AAD})/(\text{Max}|S^{xs}_{Sim}|)$ should be recognized as the main source of deviations for comparisons

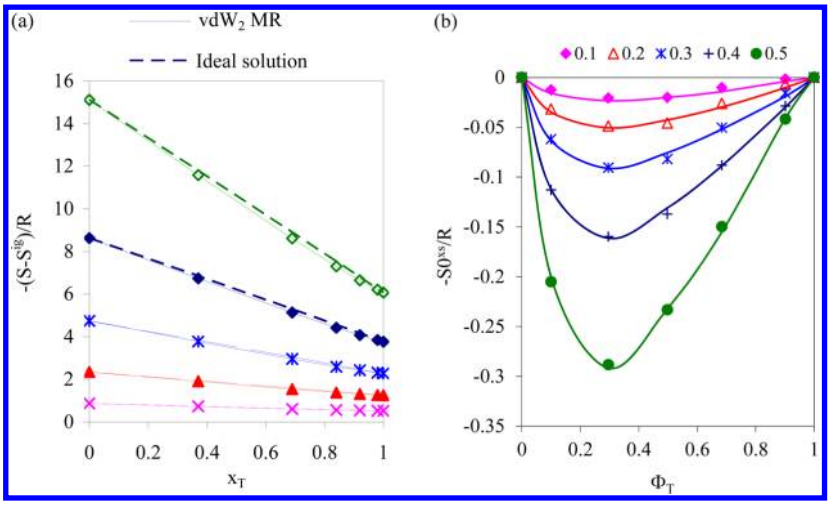

Figure 4. Entropy departure function and athermal excess entropy of mixing for toluene + PS (C_{40}) based on vdW_2 (packing fractions are listed in the legend) with $\mathcal{R}$ = 5.25 and δ_s^S/δ_p^S = 1.48.

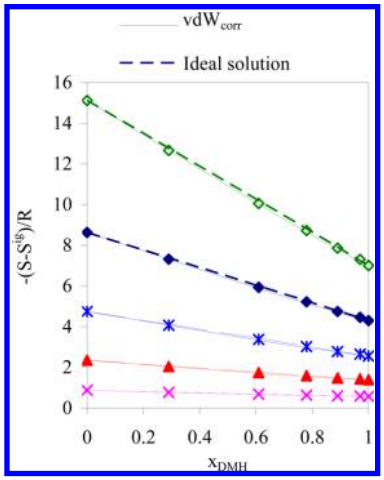

Figure 5. Entropy departure function for DMH + PS (C_{40}) based on vdW_2 MR with $\mathcal{R}$ = 3.67 and δ_s^S/δ_p^S = 1.35 at packing fractions of 0.1 (pink), 0.2 (red), 0.3 (blue), 0.4 (dark blue), and 0.5 (green).

for nonideal solutions, S_{AAD}^{xs} is the key error for ideal and nearly ideal solutions.

Figure 9 shows the quantitative behavior of vdW_{corr} with $k_{ij}^{S0} = -0.04\chi_0^S$ as given by eq 32 for a nonideal solution, i.e., methane + PE in various chain lengths. The trends are smooth despite the large amplification. For example, the athermal entropy at a packing fraction of 0.4 and carbon number of 80 is roughly 40, but the athermal excess entropy is only −8, almost 1 order of magnitude smaller. Hence, the lack of scatter in these trends is noteworthy.

The prevalence of van der Waals mixing may be reassuring for those who prefer the Flory−Huggins model with a temperature dependent χ parameter that includes a constant (athermal) term. The athermal contribution to the χ parameter would be consistent with the vdW_1 model. In that case, the vdW_{corr} model can be regarded as a predictor of the athermal χ. By limiting applications to liquids, where $\eta \sim 0.4$, it may be possible to refine the vdW_{corr} model to provide greater precision in that range. Nevertheless, it would be misleading to assume a simple power series such as $\chi = \chi_0 + \chi_1/T + \chi_2/T^2 + \ldots$ because the higher order terms would be indirectly

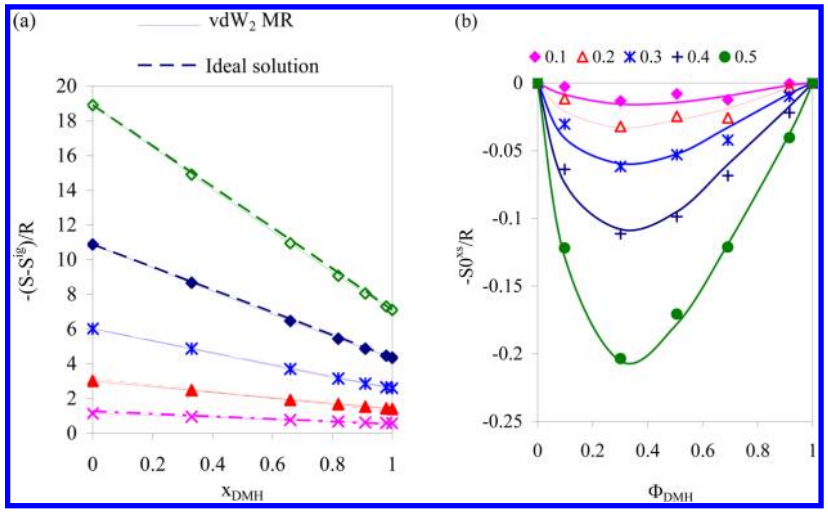

Figure 6. Entropy departure function and athermal excess entropy of mixing for DMH + PP (C_{39}) based on vdW_2 (packing fractions are listed in the legend) with $\mathcal{R}$ = 4.48 and δ_s^S/δ_p^S = 1.34.

dx.doi.org/10.1021/ma402593m | Macromolecules 2014, 47, 1514−1531

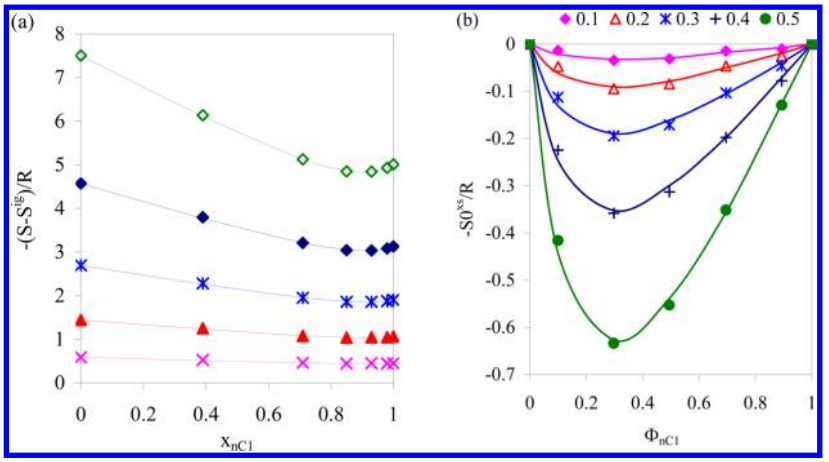

Figure 7. Entropy departure function and excess entropy for methane + PP (C_9) with based on vdW_2 MR (packing fractions are listed in the legend) $\mathcal{R}$ = 5.68 and δ_s^S/δ_p^S = 1.97.

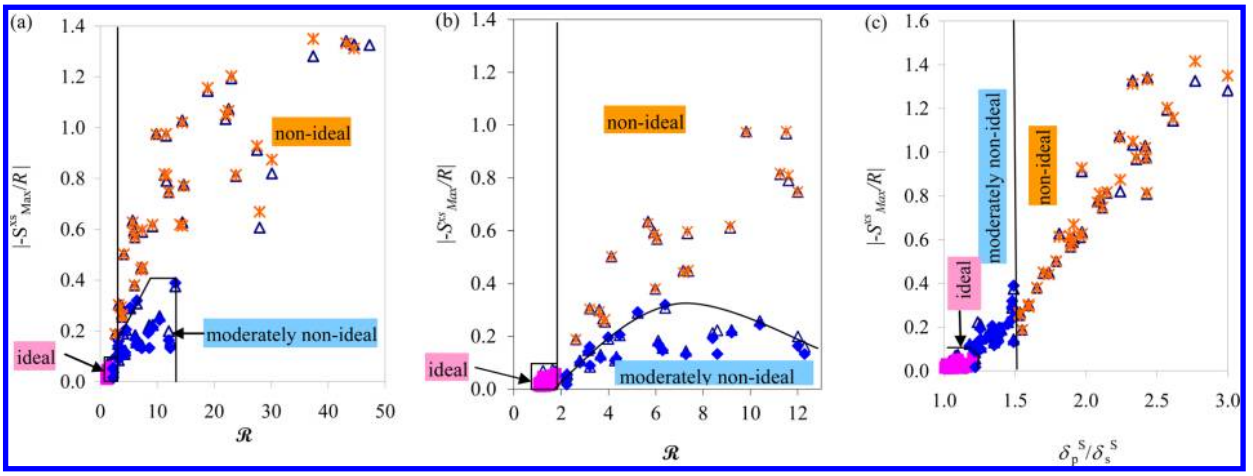

Figure 8. Phase diagram of the absolute maximum athermal excess entropy of mixing versus two key parameters ($\mathcal{R}$ and δ_s^S/δ_p^S), the hollow points are simulation data and the cross and filled points are smoothed estimates based on the vdW_2 mixing rule.

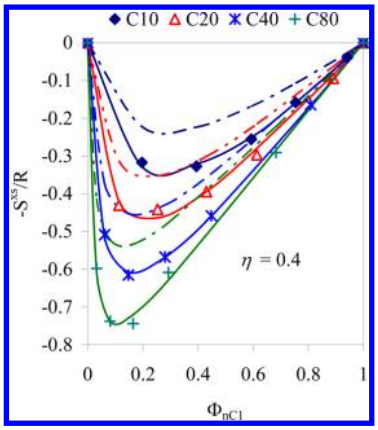

Figure 9. Athermal excess entropy of mixing for methane + PE systems based on vdW_{corr} (solid lines) and SAFT (dashed lines).

accounting for variations of χ with density, rather than temperature.

4.3. Comparisons to Alternative Models for Athermal Excess Entropy. In this subsection, accuracy has been evaluated for off-lattice molecular theories including PC-SAFT, a modified version of the simplified SAFT (Ms-SAFT), and lattice theories including FH, GS, and GCLF. PC-SAFT is representative of many implementations of the SAFT model in the way that it treats the excess entropy. The Ms-SAFT model implements an empirical modification that incorporates a single adjustable parameter. It is not predictive. The lattice theories require specification of a particular packing fraction. The GCLF model is taken as representative of lattice theories for detailed comparisons.

The PC-SAFT model provides qualitative accuracy with no adjustable parameter. Its (S^{xs} AAD)/(Max|S^{xs}_{Sim}|) is 8% for nonideal mixtures, 21% for moderately nonideal systems, and 44% for ideal systems, with overall deviations of 21%. These values compare to vdW_{corr} values of 5%, 14%, 36% with overall deviations of 16% (Table 2). While investigating the detailed data, we observed that the PC-SAFT model has larger deviations (~25% overall) in the liquid region ($0.3 < \eta < 0.5$) and lower deviations in the gas region ($0.1 < \eta < 0.3$). In general, the SAFT model tended to underestimate the nonideality slightly. To understand the nature of the SAFT model in predicting the athermal excess entropy of mixing and finding the key parameter(s) (such as $\mathcal{R}$ and δ^S in vdW), a nonideal polymer solution (ethane + hexadecane) was investigated in more detail (Figure 10). Figure 10a shows the prediction of the SAFT model with only the hard-sphere term included. Figure 10b is the SAFT model prediction with only the hard-chain term included. It is observed that the hard-chain

dx.doi.org/10.1021/ma402593m | Macromolecules 2014, 47, 1514−1531

Table 2. Summary of Simulation Data and Model Predictions for Different Mixture Volume Ratios of Polymer Solutions Based on the PC-SAFT and Ms-SAFT Theories

			PC-SAFT		Ms-SAFT			GCLF	
			S^{xs} AAD	(S^{xs} AAD)/(Max$\|S^{xs}_{Sim}\|$)	m_{ij}	S^{xs} AAD	(S^{xs} AAD)/(Max$\|S^{xs}_{Sim}\|$)	S^{xs} AAD	(S^{xs} AAD)/(Max$\|S^{xs}_{Sim}\|$)
Polymer Solutions									
Nonideal									
1	octanol	water	0.267	0.275	0.65	0.022	0.023	0.223	0.228
2	methane	isoprene	0.026	0.087	0.29	0.003	0.011	0.115	0.377
3	PE	methane	0.054	0.095	0.59	0.006	0.011	0.128	0.225
4			0.066	0.084	0.97	0.013	0.016	0.182	0.230
5			0.093	0.086	1.76	0.012	0.015	0.269	0.251
6			0.148	0.115	3.41	0.017	0.022	0.336	0.253
7		ethane	0.014	0.037	0.49	0.005	0.012	0.068	0.267
8			0.017	0.068	0.32	0.006	0.023	0.088	0.231
9			0.024	0.053	0.62	0.008	0.017	0.143	0.319
10			0.030	0.048	1.17	0.014	0.023	0.201	0.321
11			0.146	0.177	1.26	0.039	0.048	0.252	0.305
12	PIP	methane	0.054	0.091	0.58	0.007	0.011	0.181	0.305
13			0.075	0.093	1.01	0.007	0.009	0.278	0.342
14			0.095	0.092	1.81	0.008	0.009	0.346	0.335
15			0.120	0.090	3.36	0.012	0.009	0.431	0.322
16		ethane	0.016	0.060	0.31	0.005	0.020	0.083	0.310
17			0.025	0.056	0.61	0.006	0.014	0.140	0.312
18			0.040	0.065	1.20	0.010	0.016	0.202	0.330
19			0.029	0.031	2.04	0.017	0.019	0.255	0.279
20	PP	methane	0.049	0.077	0.56	0.008	0.013	0.194	0.306
21			0.076	0.074	1.20	0.005	0.006	0.326	0.317
22			0.092	0.077	1.77	0.007	0.009	0.388	0.325
23			0.090	0.068	3.09	0.014	0.019	0.418	0.315
24		ethane	0.012	0.040	0.31	0.005	0.016	0.089	0.295
25			0.023	0.038	0.81	0.004	0.007	0.183	0.299
26			0.069	0.092	1.26	0.006	0.008	0.232	0.311
27			0.025	0.031	1.85	0.016	0.020	0.260	0.316
28	PS	methane	0.046	0.092	0.44	0.005	0.011	0.276	0.139
29			0.069	0.071	0.99	0.007	0.008	0.297	0.307
30			0.087	0.076	1.47	0.010	0.011	0.346	0.562
31			0.074	0.058	2.37	0.014	0.018	0.408	0.563
32		ethane	0.013	0.070	0.22	0.005	0.028	0.058	0.310
33			0.034	0.057	0.70	0.008	0.014	0.165	0.280
34			0.029	0.039	1.05	0.006	0.008	0.217	0.291
35			0.031	0.038	1.46	0.019	0.023	0.253	0.313
	total nonideal		**0.062**	**0.077**		**0.011**	**0.015**	**0.229**	**0.308**
Moderately Nonideal									
36	PE	toluene	0.018	0.214	0.17	0.009	0.102	0.092	1.087
37			0.028	0.133	0.47	0.009	0.042	0.113	0.729
38			0.020	0.125	0.36	0.025	0.153	0.049	0.307
39		DMH	0.018	0.324	0.14	0.007	0.132	0.049	0.868
40			0.025	0.201	0.35	0.014	0.112	0.086	0.700
41			0.030	0.136	−0.09	0.035	0.158	0.112	0.504
42	PIP	toluene	0.024	0.162	0.21	0.016	0.111	0.237	0.621
43			0.077	0.422	−0.02	0.071	0.387	0.087	0.473
44			0.049	0.245	0.35	0.043	0.219	0.079	0.398
45		DMH	0.012	0.263	0.09	0.006	0.124	0.053	1.122
46			0.020	0.183	0.25	0.008	0.073	0.069	0.632
47			0.030	0.143	0.64	0.015	0.072	0.113	0.578
48	PP	toluene	0.033	0.174	0.08	0.007	0.037	0.063	0.330
49			0.041	0.132	0.67	0.013	0.043	0.088	0.286
50			0.132	0.351	−0.03	0.109	0.290	0.178	0.474
51		DMH	0.013	0.118	0.21	0.008	0.074	0.060	0.555
52			0.044	0.217	0.44	0.004	0.017	0.077	0.377
53			0.122	0.230	0.27	0.137	0.259	0.169	0.319
54	PS	toluene	0.018	0.115	0.35	0.011	0.071	0.217	1.401

dx.doi.org/10.1021/ma402593m | *Macromolecules* 2014, 47, 1514−1531

Table 2. continued

			PC-SAFT		Ms-SAFT			GCLF	
			S^{xs} AAD	(S^{xs} AAD)/(Max$\|S^{xs}_{Sim}\|$)	m_{ij}	S^{xs} AAD	(S^{xs} AAD)/(Max$\|S^{xs}_{Sim}\|$)	S^{xs} AAD	(S^{xs} AAD)/(Max$\|S^{xs}_{Sim}\|$)
			Polymer Solutions						
			Nonideal						
			Moderately Nonideal						
55			0.017	0.059	0.49	0.005	0.017	0.277	0.962
56			0.053	0.204	0.50	0.063	0.243	0.187	0.725
57		DMH	0.021	0.374	0.04	0.024	0.429	0.057	1.039
58			0.017	0.129	0.32	0.016	0.126	0.064	0.489
59			0.054	0.377	0.03	0.026	0.178	0.095	0.657
	total moderately nonideal		**0.038**	**0.210**		**0.028**	**0.145**	**0.111**	**0.651**
			Ideal						
60	PE	toluene	0.013	0.431	0.06	0.008	0.252	0.118	2.425
61		DMH	0.007	0.332	0.02	0.007	0.320	0.044	1.544
62	PIP	toluene	0.010	0.131	−0.04	0.009	0.130	0.244	0.803
63		DMH	0.008	0.365	0.03	0.008	0.344	0.051	2.336
64	PP	toluene	0.010	0.267	0.02	0.009	0.262	0.046	1.418
65		DMH	0.013	0.619	−0.04	0.011	0.504	0.065	3.031
66	PS	toluene	0.009	0.224	0.04	0.010	0.229	0.123	2.953
67		DMH	0.020	1.714	−0.12	0.010	0.835	0.206	2.957
68	ACN	*trans*-2-butene	0.006	0.246	0.04	0.003	0.135	0.025	0.962
69		*cis*-2-butene	0.005	0.242	0.04	0.004	0.197	0.054	2.700
70		1,3-butadiene	0.004	0.311	0.02	0.003	0.264	0.027	1.929
71	ethanol	R-227	0.007	0.105	0.08	0.006	0.094	0.108	1.612
72	DMF	*trans*-2-butene	0.007	0.483	−0.03	0.004	0.272	0.034	2.267
73		*cis*-2-butene	0.004	0.205	−0.02	0.004	0.201	0.046	2.091
74		1,3-butadiene	0.006	0.463	−0.02	0.004	0.315	0.029	2.231
75	butane	perfluoroC_4	0.009	0.560	−0.02	0.006	0.385	0.017	1.133
76	hexane	butanol	0.011	0.391	0.03	0.010	0.377	0.052	1.926
77	C_4amine	propanol	0.013	0.896	−0.02	0.007	0.501	0.061	4.067
78		butanol	0.007	0.277	0.04	0.005	0.228	0.052	2.167
79	octanol	3-MeC_5OH	0.009	0.402	−0.08	0.005	0.224	0.055	2.391
80		3C_5amine	0.007	0.424	−0.03	0.005	0.304	0.048	2.824
81		hexane	0.016	0.475	−0.01	0.015	0.464	0.081	2.455
	total ideal		**0.009**	**0.435**		**0.007**	**0.311**	**0.072**	**2.192**
	total		**0.040**	**0.214**		**0.015**	**0.134**	**0.152**	**0.922**

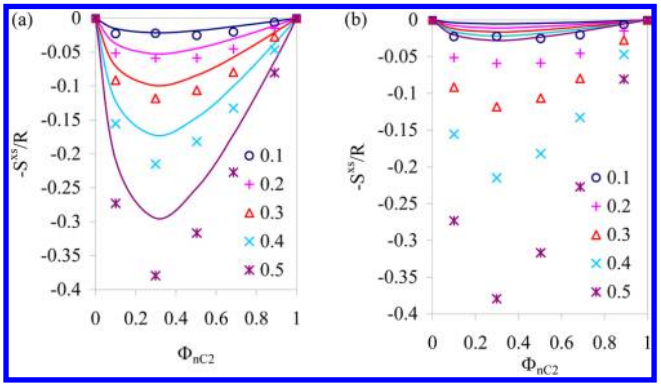

Figure 10. Athermal excess entropy of mixing for ethane + PE (C_{16}) system based on hard-sphere (a) and hard chain term (b) of the SAFT theory (packing fractions are listed in the legend) with $\mathcal{R}$ = 5.98 δ_s^S/δ_p^S = 1.65.

contribution had a very small impact on the excess entropy. This is because of the equivalent hard sphere diameter ratio parameter for the SAFT model, which basically plays the role of both $\mathcal{R}$ and δ^S for the equation of state. In this "polymer" solution (ethane + hexadecane), the equivalent segment diameter ratio is roughly 1.3.

The Ms-SAFT equation uses one interaction parameter per mixture and provides a similar correlation to the VdW_1 model. For Ms-SAFT the (S^{xs} AAD)/(Max$\|S^{xs}_{Sim}\|$) ratio is 1.5% for nonideal solutions, 15% for moderately nonideal systems, and 31% for ideal systems, with an overall deviation of 13%. These values compare to 4%, 12%, and 28%, with an overall deviation of 13% for the VdW_1 model. In general, this relatively simple modification of the SAFT model can provide nearly quantitative results.

Figure 11 illustrates the trends for several lattice theories. The results for these mixtures are typical of all mixtures. In general, the GS, FH, and GCLF lattice theories exhibit excess skewness toward the low composition range of solvent. They also tend to underestimate excess entropy at a packing fraction of 0.5. The underestimation would be less at a packing fraction of 0.3, but the skewness would still be inaccurate. In general, we find little support for the lattice theories based on our simulations. The Blanks and Prausnitz (B&P) model tends to overestimate the nonideality, although skewness is reasonable. A value of χ^S = 0.35 was used in evaluating this approach.

5. CONCLUSIONS

We find that the excess entropy of mixing is dominated by the influence of pure component entropy density. The effects of

dx.doi.org/10.1021/ma402593m | *Macromolecules* 2014, 47, 1514−1531

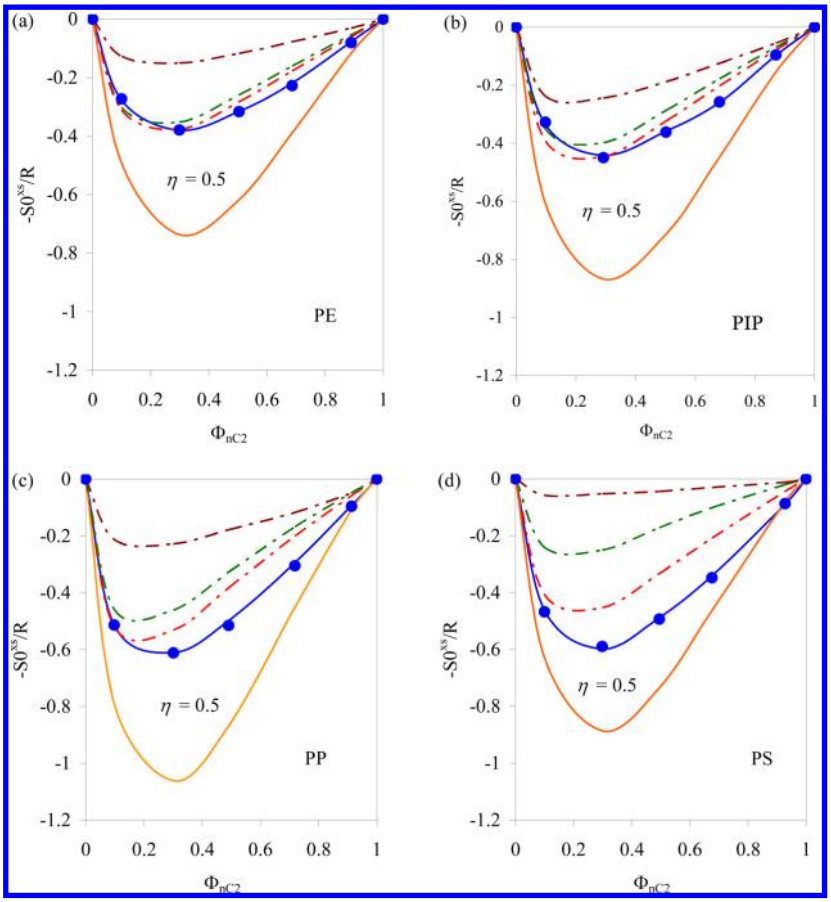

Figure 11. Athermal excess entropy of mixing for (a) ethane + PE (C_{16}), (b) ethane + PIP (C_{20}), (c) ethane + PP (C_{24}), and (d) ethane + PS (C_{24}). vdW-2 model (solid blue line), GS (dashed green line), FH (dashed red lines), B&P (solid orange lines), and GCLF (dashed brown lines) theories at $\eta = 0.5$.

molecular details like branching and rings are remarkably small. These effects have been evaluated using the DMD method with hard core potential models such that the inferred entropy of mixing is athermal, with no interference from attractive contributions or softness of the potential. The DMD method is uniquely suited to this study because it provides a direct and precise measure of the pressure, which can then be transformed to entropy through thermodynamic integration. We provide the entire database of our simulation results as Supporting Information and welcome alternative compilations or interpretations of similar data. Overall, the excess entropy of mixing at constant packing fraction is positive, indicating that mixing is more favorable than would be expected based on the ideal solution model. This is also reflected by negative deviations from nonideality in pressure vs composition as illustrated in Figure 2.

Our analysis shows that van der Waals mixing provides a quantitative basis for correlating the behavior for all chain lengths and molecular shapes. Furthermore, the χ_{ij}^{S} parameter can be correlated in terms of a measure of entropy density related to solubility parameter. The resulting trends in mixture entropy vs molecular weight show a fairly tight pattern that supports the predictability that we observe, as illustrated in Figure 8.

Alternative theories provide mixed results when compared to the simulation data. SAFT models provide reasonable predictions when based on Chapman's original formulation with the BMCSL model as a basis. It is possible that these SAFT models are more accurate for real mixtures than what is represented in our study, because the SAFT temperature dependence of the effective repulsive diameter leads to ambiguity when comparing to athermal systems. Our resolution of this ambiguity does not represent any effort to optimize SAFT models in this regard. Lattice models, on the other hand, did not compare favorably to our simulation results, whether they included void spaces or not. Possibly, this is a result of misrepresenting the ideal gas reference state at constant pressure, but the lattice results would grossly underestimate the excess entropy of mixing if that were taken into account. In general, none of the lattice models that we considered were consistent with the prevalence of van der Waals mixing that we observed.

The imposition of constant packing fraction throughout our analysis is a significant consideration that should not be overlooked. As shown in Figure 2, the pressure is lower than the ideal value when mixed at constant packing fraction. This means that the packing fraction would need to be increased in order to maintain constant pressure. Increasing the packing fraction reduces the volume such that the excess entropy at constant pressure is actually of the opposite sign. The exact behavior at constant pressure is complicated by the influence of the equation of state, which may have its own imprecision, so considering the problem at constant pressure might not lead to the relatively simple trends observed in our analysis.

To the extent that some mixtures exhibit significant deviations from the Flory–Huggins model, the root causes

dx.doi.org/10.1021/ma402593m | *Macromolecules* 2014, 47, 1514–1531

should be sought in effects that have been neglected in our analysis. Conformational[71] behavior is fairly simple in our model compounds. Hydrogen bonding or other localized forms of energy would not be athermal, so they are beyond the scope of our analysis. When such causes are conjectured, however, it is essential that they be supported by off-lattice molecular simulations. The complex interactions between composition, pressure, temperature, and density can lead to cancellations of errors that are misleading when the conjectured models are compared directly to experimental data.

■ ASSOCIATED CONTENT

Supporting Information

Mixture repulsive compressibility factor for different systems along with excess entropy of mixing for mixture of solvents. This material is available free of charge via the Internet at http://pubs.acs.org/.

■ AUTHOR INFORMATION

Corresponding Author

*(J.R.E.) Telephone: 330-972-7253. Fax: 330-972-5856. E-mail: jelliott@uakron.edu.

Notes

The authors declare no competing financial interest.

■ ACKNOWLEDGMENTS

The authors are grateful to Prof. Ronald P. Danner from Penn State University, University Park, PA, Prof. Walter G. Chapman, Rice University, Houston, TX, and Prof. Joachim Gross from Technical University of Stuttgart, Germany, for their erudite scientific discussions and distributing the UNIFAC-FV, SAFT, and PC-SAFT codes. This work was supported in part by National Science Foundation Grant CTS-0226532 and by ChemStations Inc., Houston, TX.

■ REFERENCES

(1) Breslow, R.; Tirrell, M. V., *Beyond the Molecular Frontier - Challenges for Chemistry and Chemical Engineering*. The National Academies Press: Washington, DC, 2003; p 224.
(2) Guggenheim, E. A. *Proc. R. Soc.* **1944**, *183 A*, 203−212.
(3) Guggenheim, E. A., *Mixtures*; Oxford University Press: New York, 1952.
(4) Oishi, T.; Prausnitz, J. M. *Ind. Eng. Chem. Process Des. Dev.* **1978**, *17* (3), 333−339.
(5) Panayiotou, C. P.; Vera, J. H. *Polym. J.* **1984**, *16*, 89.
(6) Lindvig, T.; Economou, I. G.; Danner, R. P.; Michelsen, M. L.; Kontogeorgis, G. M. *Fluid Phase Equilib.* **2004**, *220* (1), 11−20.
(7) Flory, P. J., *Statistical Mechanics of Chain Molecules*; Interscience: New York, 1969.
(8) Danner, R. P.; High, M. S., *Handbook of Polymer Solution Thermodynamics*; AIChE: New York, 1993.
(9) Alawneh, M.; Henderson, D. *Mol. Phys.* **2008**, *106* (5), 607−614.
(10) Santos, A.; Yuste, S. B.; de Haro, M. L.; Alawneh, M.; Henderson, D. *Mol. Phys.* **2009**, *107* (7), 685−691.
(11) Mansoori, G. A.; Carnahan, N. F.; Starling, K. E.; Leland, T. W. *J. Chem. Phys.* **1971**, *54*, 1523−1525.
(12) Gray, N. H.; Elliott, J. R. In *Quadratic Mixing in Perturbation Theory*; Presented at the AIChE Fall National Meeting, Austin, TX, 2004; AIChE: New York, 2004; p 160e.
(13) Vahid, A.; Sans, A. D.; Elliott, J. R. *Ind. Eng. Chem. Res.* **2008**, *47*, 7955−7964.
(14) Dzugutov, M. *Nature* **2001**, *411* (6838), 720−720.
(15) Rosenfeld, Y. Quasi-universal scaling law for atomic transport in simple fluids. *J. Phys. IV Fr.* **2000**, *10*, 129−134.
(16) Rosenfeld, Y. *J. Phys. Condens. Matter* **1999**, *11* (28), 5415−5427.
(17) Ghobadi, A. F.; Elliott, J. R. *J. Chem. Phys.* **2013**, *139*, 234104.
(18) Gerek, Z. N.; Elliott, J. R. *Ind. Eng. Chem. Res.* **2010**, 3411−3423.
(19) Prausnitz, J. M.; Lichtenthaler, R. N.; Gomez de Azevedo, E., *Molecular Thermodynamics of Fluid-Phase Equilibria*, 3rd ed.; Prentice-Hall PTR: Upper Saddle River, NJ, 1999.
(20) Elliott, J. R.; Vahid, A.; Sans, A. D. *Fluid Phase Equilib.* **2006**, *256*, 4−13.
(21) Dos Ramos, M. C.; Blas, F. J. *J. Phys. Chem. B* **2005**, *109*, 12145−12153.
(22) Danner, R. P.; Hamedi, M. *Abstr. Pap. Am. Chem. Soc.* **2000**, *219*, 105−IEC.
(23) Guggenheim, E. A., *Applications of Statistical Mechanics*; Oxford University Press: New York, 1972.
(24) Boublik, T. *J. Chem. Phys.* **1970**, *53*, 471−472.
(25) Chapman, W. G.; Gubbins, K. E.; Jackson, G.; Radosz, M. *Fluid Phase Equilib.* **1989**, *52*, 31.
(26) Prigogine, I. *The Molecular Theory of Solutions*; North Holland: Amsterdam, 1957.
(27) Flory, P. A. J.; Orwoll, R. A.; Vrij, A. *J. Am. Chem. Soc.* **1964**, *86*, 3507.
(28) Beret, S.; Prausnitz, J. M. *AIChE J.* **1975**, *21*, 1123.
(29) Lacombe, R. H.; Sanchez, I. C. *J. Phys. Chem.* **1976**, *80* (23), 2568−2580.
(30) Sanchez, I. C.; Lacombe, R. H. *J. Phys. Chem.* **1976**, *80*, 2352.
(31) Sanchez, I. C.; Lacombe, R. H. *Macromolecules* **1978**, *11* (6), 1145−1156.
(32) Costas, M.; Epstein, H. I.; Sanctuary, B. C.; Richon, D.; Renon, H. *J. Phys. Chem.* **1981**, *85* (9), 1264−1266.
(33) Costas, M.; Sanctuary, B. C. *Fluid Phase Equilib.* **1984**, *18* (1), 47−60.
(34) Costas, M.; Sanctuary, B. C. *J. Phys. Chem.* **1981**, *85* (21), 3153−3160.
(35) Simha, R.; Somcynsky, T. *Macromolecules* **1969**, *2* (4), 342−350.
(36) Sandler, S. I., *Chemical, Biochemical, and Engineering Thermodynamics*; 4th ed.; Wiley: New York, 2006.
(37) Scatchard, G. *Chem. Rev.* **1931**, 321−333.
(38) Hildebrand, J. H.; Prausnitz, J. M.; Scott, R. L., *Regular and Related Solutions*; Van Nostrand-Reinhold: New York, 1970.
(39) Blanks, R. F.; Prausnitz, J. M. *Ind. Eng. Chem. Res.* **1964**, *3*, 1−8.
(40) Small, P. A. *J. App. Chem.* **1953**, *3*, 71−80.
(41) Orbey, H.; Sandler, S. I., *Modeling vapor-liquid equilibria: cubic equations of state and their mixing rules*; Cambridge University Press: New York, 1998; p 207.
(42) Sengers, J. V.; Kayser, R. F.; Peters, C. J.; White, H. J., *Equations of State for Fluids and Fluid Mixtures*, 1st ed.; Elsevier: Amsterdam, 2000.
(43) Rubinstein, M.; Colby, R. H., *Polymer Physics*; Oxford: New York, 2003.
(44) Flory, P. J., *Principles of Polymer Chemistry*, 1st ed.; Cornell University Press: New York, 1953.
(45) Jones, A. T.; Derawi, S.; Danner, R. P.; Duda, J. L. *Fluid Phase Equilib.* **2007**, *259* (1), 116−122.
(46) Jones, A. T.; Zielinski, J. M.; Danner, R. P. *Fluid Phase Equilib.* **2009**, *280* (1−2), 88−93.
(47) Danner, R. P.; Daubert, T. E. *Manual for predicting chemical process design data: data prediction manual/Design Institute for Physical Property Data, American Institute of Chemical Engineers*; American Institute of Chemical Engineers: New York, 1983.
(48) Gross, J.; Sadowski, G. *Ind. Eng. Chem. Res.* **2001**, *40*, 1244−1260.
(49) Elliott, J. R.; Natarajan, R. N. *Ind. Chem. Eng. Res.* **2002**, *41*, 1043.
(50) Tihic, A. K.; Kontogeorgis, G. M.; von Solms, N.; Michelsen, M. L. *Fluid Phase Equilib.* **2006**, *248*, 29−43.
(51) Tihic, A.; Von Solms, N.; Michelsen, M. L.; Kontogeorgis, G. M.; Constantinou, L. *Fluid Phase Equilib.* **2009**, *281* (1), 60−69.

(52) Tihic, A.; Von Solms, N.; Michelsen, M. L.; Kontogeorgis, G. M.; Constantinou, L. *Fluid Phase Equlib.* **2009**, *281* (1), 70−77.
(53) Tihic, A.; Kontogeorgis, G. M.; von Solms, N.; Michelsen, M. L.; Constantinou, L. *Ind. Eng. Chem. Res.* **2008**, *47* (15), 5092−5101.
(54) Unlu, O.; Gray, N. H.; Gerek, Z. N.; Elliott, J. R. *Ind. Eng. Chem. Res.* **2004**, *43*, 1788−1793.
(55) Barker, J. A.; Henderson, D. *J. Chem. Phys.* **1967**, *47*, 2856.
(56) Martin, M. G. MCCCS Towhee. http://towhee.sourceforge.net/
(57) Vahid, A.; Elliott, J. R. *AIChE J.* **2010**, *56* (2), 485−505.
(58) Ghobadi, A. F.; Elliott, J. R. *Fluid Phase Equilib.* **2011**, *306*, 57−66.
(59) Vahid, A.; Elliott, J. R. *Fluid Phase Equilib.* **2013**, *351*, 61−68.
(60) Elliott, J. R.; Gray, N. H. *J. Chem. Phys.* **2005**, *123*, 184902.
(61) Rosenfeld, Y. *Phys. Rev. A* **1977**, *15*, 2545.
(62) Noid, W. G.; Liu, P.; Wang, Y.; Chu, J. W.; Ayton, G. S.; Izvekov, S.; Anderson, H. C.; Voth, G. A. *J. Chem. Phys.* **2008**, *128*, 244115.
(63) Sun, X.; Gezelter, J. D. *Phys. Rev. E.* **2007**, *75*, 031602.
(64) Press, W. H.; Teukolsky, S. A.; Vetterling, W. T.; Flannery, B. P. *Numerical Recipes: The Art of Scientific Computing*; Cambridge University Press: New York, 2007.
(65) Garbow, B. S.; Hillstrom, K. E.; More, J. J. *MINPACK Project*; Argonne National Laboratory: Chicago, IL, 1980.
(66) Emami, F. S.; Vahid, A.; Elliott, J. R. *J. Chem. Thermodyn.* **2009**, *41*, 530−537.
(67) Elliott, J. R.; Vahid, A.; Sans, A. D. *Fluid Phase Equilb.* **2007**, *256*, 4−13.
(68) Baskaya, F. S.; Gray, N. H.; Gerek, Z. N.; Elliott, J. R. *Fluid Phase Equilb.* **2005**, *236*, 42−52.
(69) Gray, N. H.; Gerek, Z. N.; Elliott, J. R. *Fluid Phase Equilib.* **2005**, *228−229C*, 147−153.
(70) Mathias, P. M.; Elliott, J. R.; Klamt, A. *Ind. Eng. Chem. Res.* **2008**, *47*, 4996−5004.
(71) Öttinger, H. C. *Beyond Equilibrium Thermodynamics*, 1st ed.; John Wilcy & Sons: Hoboken, NJ, 2005.